

SECOND VIRIAL COEFFICIENTS
OF
SEVERAL POLAR-NONPOLAR BINARY MIXTURES

By
DAVID HARRISON KNOEBEL

Bachelor of Science
Michigan Technological University
Houghton, Michigan
1961

Master of Science
Oklahoma State University
Stillwater, Oklahoma
1964

Submitted to the Faculty of the Graduate
School of the Oklahoma State
University in partial fulfillment of
the requirements for
the degree of
DOCTOR OF PHILOSOPHY
May, 1967

JAN 12 1968

SECOND VIRIAL COEFFICIENTS
OF
SEVERAL POLAR-NONPOLAR BINARY MIXTURES

Thesis Approved:

Wayne C. Edmister
Thesis Adviser

John B. West

K. C. Chao

D. D. Durkin
Dean of the Graduate College

659307

PREFACE

In this study second virial coefficients are determined from low pressure experimental PVT data for a number of binary mixtures containing a polar and a nonpolar component. The interaction second virial coefficients are calculated and compared with results obtained using potential functions.

I would like to express my gratitude to the members of my Doctoral Committee and the entire staff and graduate students of the School of Chemical Engineering for their help in my graduate studies. I am particularly grateful to Professor W. C. Edmister, my thesis adviser, and to Professor K. C. Chao who guided my work during the final year. I would also like to express my appreciation to Mrs. Mary Fuller for her help in typing this thesis.

Financial aid, which has been gratefully received, has come from a National Defense Education Act Fellowship, a Petroleum Research Fund Fellowship, and teaching and research assistantships from Oklahoma State University.

TABLE OF CONTENTS

Chapter	Page
I. INTRODUCTION	1
II. LITERATURE	3
Experimental Data	3
Theoretical Treatment	4
Lennard-Jones Potential	9
Stockmayer Potential	10
Kihara Potential	10
III. APPARATUS DESCRIPTION	12
Piezometer	12
Sample Injection	13
Materials	15
IV. EXPERIMENTAL PROCEDURE	17
V. EXPERIMENTAL RESULTS	21
VI. THEORETICAL TREATMENT OF RESULTS	36
VII. DISCUSSION OF RESULTS	45
Experimental Results	45
Theoretical Results	53
VIII. CONCLUSIONS AND RECOMMENDATIONS	58
SELECTED BIBLIOGRAPHY	61
APPENDIX A	64
APPENDIX B	69

Chapter	Page
APPENDIX C	83
APPENDIX D	88
APPENDIX E	104

LIST OF TABLES

Table	Page
I. Summary of Experimental Results for Benzene-Methanol Systems	26
II. Summary of Experimental Results for Benzene-Ethanol Systems	27
III. Summary of Experimental Results for Benzene-Acetone Systems	28
IV. Summary of Experimental Results for Benzene-Diethyl Ether Systems	29
V. Parameters for the Kihara Potential	37
VI. Parameters for the Stockmayer Potential	39
VII. Mixture Potential Parameters	40
VIII. Interaction Second Virial Coefficients	42
A-I. Water Calibration of Bulb Volumes	67
A-II. Volume Ratios From Argon Calibration	67
A-III. Comparison of Water and Argon Calibration	68
B-I. Example of Experimental Data	70
B-II. Results for Benzene	74
B-III. Results for Methanol	75
B-IV. Results for Ethanol	76

Table	Page
B-V. Results for Acetone	77
B-VI. Results for Diethyl Ether	78
B-VII. Results for Benzene-Methanol Systems . . .	79
B-VIII. Results for Benzene-Ethanol Systems	80
B-IX. Results for Benzene-Acetone Systems	81
B-X. Results for Benzene-Diethyl Ether Systems .	82
C-I. Results of B_{12} Calculations for the Benzene-Methanol System	84
C-II. Results of B_{12} Calculations for the Benzene-Ethanol System	85
C-III. Results of B_{12} Calculations for the Benzene-Acetone System	86
C-IV. Results of B_{12} Calculations for the Benzene-Diethyl Ether System	87
D-I. Error Analysis Results for Benzene Data . .	90
D-II. Error Analysis Results for Methanol Data .	91
D-III. Error Analysis Results for Ethanol Data . .	92
D-IV. Error Analysis Results for Acetone Data . .	93
D-V. Error Analysis Results for Diethyl Ether Data	94
D-VI. Error Analysis Results for Benzene- Methanol Data	95
D-VII. Error Analysis Results for Benzene- Ethanol Data	96
D-VIII. Error Analysis Results for Benzene- Acetone Data	97

Table	Page
D-IX. Error Analysis Results for Benzene- Diethyl Ether Data	98

LIST OF FIGURES

Figure	Page
1. Potential Energy Versus Separation Distance	9
2. Low Pressure PVT Apparatus	14
3. Second Virial Coefficients of Benzene Versus Temperature	22
4. Second Virial Coefficients of Methanol as a Function of Temperature	23
5. Second Virial Coefficients of Ethanol as a Function of Temperature	24
6. Second Virial Coefficients of Acetone and Diethyl Ether as a Function of Temperature	25
7. Second Virial Coefficients of the Benzene-Methanol System Versus Composition	31
8. Second Virial Coefficients of the Benzene-Ethanol System Versus Composition	32
9. Second Virial Coefficients of the Benzene-Acetone System Versus Composition	33
10. Second Virial Coefficients of the Benzene-Diethyl Ether System Versus Composition	34
11. Temperature Dependence of the Interaction Second Virial Coefficients	35
12. Typical Plot of PV Versus P	46

Figure	Page
13. Behavior of PV Versus P Relationship when Adsorption is Present	48
14. Vapor Pressure Versus Temperature	49
D-1. Expected Deviation in PV as a Function of Pressure	101
D-2. Average Expected Percent Deviation in PV of Eight Measurements Versus the Magnitude of PV	102

CHAPTER I

INTRODUCTION

Modern state theories of matter are based upon a microscopic view which is dependent on intermolecular interactions. Through the statistical mechanical treatment of the forces between two molecules in a gas one can derive the virial equation of state. In formulating a potential energy function to describe the energy of interaction of molecules in a gas at low density only long range forces are important. The two most important of these are the dispersion forces (due to definite electron configuration which cause instantaneous dipoles to be formed) and dipole forces (due to the interaction of the permanent dipoles of polar molecules). In binary systems containing a polar and a nonpolar component there is also an interaction energy arising from dipole-induced dipole forces.

These latter systems have not been thoroughly investigated. This study was undertaken to obtain experimentally second virial coefficients for systems of this type and to examine the intermolecular potential energy functions which could be applied to them.

The experimental investigation was carried out at low

pressures (below the vapor pressure of any substance used) and over a temperature range of 40°C to 100°C. The binary systems chosen were benzene-methanol, benzene-ethanol, benzene-acetone and benzene-diethyl ether. Benzene is the nonpolar constituent and the second component is the polar constituent in these binary systems.

An apparatus previously described by the author (21) was modified such that experimental PVT data could be obtained. The apparatus was built such that data could be obtained for both mixtures and pure components.

The potential functions used in various phases of this study include the Lennard-Jones 6-12 (16), the Stockmayer (35) and the Kihara (20). Various mixing rules were applied to the pure component intermolecular parameters to determine the mixture parameters. These parameters were then used in the potential functions to calculate the interaction second virial coefficients.

CHAPTER II

LITERATURE SURVEY

In previous work (21), the author discussed the various types of apparatus which have been used to obtain experimental second virial coefficients at low pressures. Therefore a survey of experimental techniques will not be presented here.

Experimental Data

A survey of the literature was made to find existing data for second virial coefficients of binary mixtures containing a polar and a nonpolar component. Michels and coworkers (28) determined the second virial coefficients for the nitrogen-carbon dioxide, hydrogen-carbon dioxide and hydrogen carbon monoxide systems at 25°C. Methane, ethane, ethylene and helium in mixtures with carbon dioxide have also been investigated (7,37). There are volumetric data available on several other systems of this type (37). These include the propane, butane and nitrogen mixtures with carbon dioxide. The second virial coefficients have recently been reduced from the volumetric data available for these systems (17). These systems are composed of

relatively simple molecules. The unlike molecule interactions of these systems are therefore similar to the interactions of nonpolar molecules.

Several binary systems containing more complex molecules have been studied by Lambert and coworkers (10,26). These systems include n-hexane-chloroform, n-hexane-diethyl ether, cyclohexane-acetone, cyclohexane-diethyl amine and cyclohexane-acetonitrile at two temperatures. The benzene-chloroform and carbon tetrachloride-chloroform systems have also been investigated (11).

The systems of relatively simple molecules mentioned above have been analyzed as part of a study on nonpolar-nonpolar binaries (17). An empirical corresponding states law and modified mixing rules for the unlike molecule interaction were used in that study. Good agreement was obtained between the empirical and experimental values.

Theoretical Treatment

The virial equation of state has theoretical significance in that the virial coefficients are related to the interactions of molecules. The second virial coefficient accounts for two body interactions and the third virial coefficient accounts for three body interactions. The virial equation of state can be written in two different forms:

The Leiden form

$$PV = RT(1 + B/V + C/V^2 + \dots) \quad (1)$$

The Berlin form

$$PV = RT + B'P + C'P^2 + \dots \quad (2)$$

where B is equal to B' and C' equals $(C - B^2)/RT$. In this study at low pressures only the second virial coefficient is important. From statistical mechanics the second virial coefficient of a mixture is given by:

$$B_m = x^2 B_{11} + 2x(1-x)B_{12} + (1-x)^2 B_{22} \quad (3)$$

where B_m is the second virial coefficient of the mixture, x is the mole fraction of substance 1, B_{11} and B_{22} are the second virial coefficients accounting for like molecule pair interaction of component 1 and 2 respectively, and B_{12} accounts for the pair interaction of unlike molecules 1 and 2.

Second virial coefficients can be calculated using a principle of corresponding states. A law of corresponding states can be expressed either in terms of the classical reduced temperature, T/T_c , or as a function of intermolecular parameters obtained from statistical mechanical treatment. The conditions for a two parameter principle of corresponding states to hold have been summarized by Pitzer (30) as follows:

- 1) The molecules are spherically symmetrical,

either structurally or by virtue of rapid and free rotation.

- 2) The potential energy of assembly is only a function of various intermolecular distances.
- 3) The potential energy for a pair of molecules can be written as $E = A \varphi(R/R_0)$ where φ is a universal function, R is the intermolecular distance and A and R_0 are constants to be specified for each substance.

It is known that polar molecules do conform to a principle of corresponding states at higher temperatures. Therefore it is possible to infer that the molecules are spinning so rapidly that condition (1) above is fulfilled. However polar molecules are usually represented by a corresponding states equation which has an addition term which accounts for dipole interaction.

Empirical corresponding state correlations have been used with success to correlate second virial coefficients of nonpolar substances and their mixtures (13,17,31). A correlation of this type has also been shown to be applicable with appropriate mixing rules to slightly polar substances in binary mixtures with nonpolar substances (17).

Lambert (22) proposed the use of an empirical corresponding state correlation to calculate the nonpolar contribution to the second virial coefficient of polar substances. He then assumed an association constant due to molecular association to account for the difference between the nonpolar contribution and the observed second virial coefficient. This is expressed by the following

equation:

$$B = B_{(np)} - RTK_p \quad (4)$$

where K_p is the association constant, B is the observed second virial coefficient, and $B_{(np)}$ is the nonpolar contribution to the second virial coefficient calculated using the Berthelot equation of state:

$$B = 9/128 \frac{RT_c}{P_c} \left(1 - \frac{6T_c^2}{T^2} \right) \quad (5)$$

The association constant can be represented by the following equation:

$$-R \ln K_p = -\Delta H/T + \Delta S^\circ \quad (6)$$

where ΔH is an energy factor related to the depth of the potential energy trough and ΔS° is an entropy factor representing restrictions imposed on mutual orientations for the interaction to be different from nonpolar interaction. Thermal conductivity measurements have been made on polar vapors to justify the existence of association between polar molecules (23,24). The validity of this approach has been thoroughly discussed by Rowlinson (32).

The alternate approach is to use a principle of corresponding states based on statistical mechanics. From the statistical mechanical treatment of isolated pair interaction the following expression can be

derived:

$$B(T) = - \frac{N}{4} \int_0^{\infty} \int_0^{2\pi} \int_0^{\pi} \int_0^{\pi} [\exp(-\Psi/kT) - 1] \sin\theta_1 d\theta_1 \cdot \sin\theta_2 d\theta_2 d(\phi_2 - \phi_1) r^2 dr \quad (7)$$

where Ψ is the potential function for an isolated pair of molecules and in general is a function of r , the distance between the two molecules, of θ_1 and θ_2 , the angles made by the molecules in relation to the line joining their centers and of $\phi_2 - \phi_1$, the angle between the planes which pass through the line of centers and contain the two axes; N is Avogadro's number; and k is Boltzman's constant. For nonpolar molecules which are spherically symmetrical (condition 1) the potential energy has such a slight orientation dependence that an average is taken. The integration is then performed over one variable only. In this case $B(T)$ is given by the following equation:

$$B(T) = 2N\pi \int_0^{\infty} [1 - \exp(-\Psi/kT)] r^2 dr \quad (8)$$

The potential functions appearing in Equations 7 and 8 represent the potential energy between two molecules. The forces which are important in determining the potential energy are long range or Van der Waals intermolecular forces. The most important of these are the dispersion, electrostatic and induction forces.

A typical potential energy versus distance of separation is shown in Figure 1.

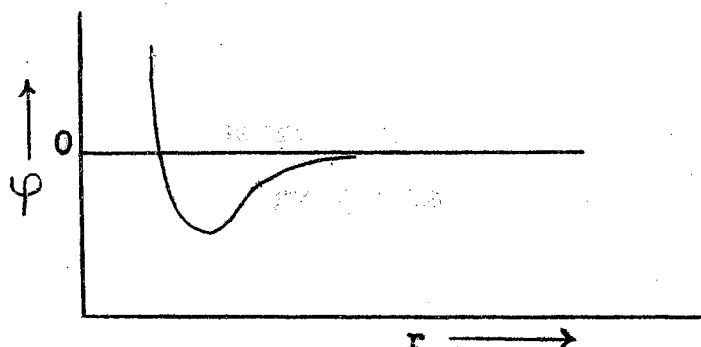


Figure 1. Potential Energy versus Separation Distance

The potential functions which have been used in the calculation of second virial coefficients are basically empirical (due to the manner in which the parameters are calculated) but use intermolecular force theory as a basis. Three widely used potential functions are discussed in the following paragraphs.

Lennard-Jones 6-12 Potential

The Lennard-Jones potential function (16) was derived for spherical soft core molecules. A soft core molecule is one which can be interpenetrated if the energies are high enough. This potential has been used with success to calculate the second virial coefficients of nonpolar molecules and especially nonpolar spherical molecules. The Lennard-Jones potential energy function is given by the following equation:

$$\psi(r) = 4\epsilon \left\{ \left(\frac{\sigma}{r}\right)^{12} - \left(\frac{\sigma}{r}\right)^6 \right\} \quad (9)$$

where σ is the value of r where $\Psi(r) = 0$, ϵ is the maximum energy of attraction, $(\sigma/r)^6$ is the attraction contribution and $(\sigma/r)^{12}$ is the repulsive contribution to the energy.

Stockmayer Potential

This potential was developed for spherical molecules with permanent dipoles at their centers (35). The Stockmayer potential has been used quite extensively in treating simple polar molecules where dipole-quadrupole and higher multipole interactions are not important. The potential energy is given by the following:

$$\Psi = 4\epsilon \left[(\sigma/r)^{12} - (\sigma/r)^6 \right] - (\mu^2/r^3)g(\theta_1, \theta_2, \phi_2 - \phi_1) \quad (10)$$

where $g(\theta_1, \theta_2, \phi_2)$ is the angular dependence of the dipole-dipole interaction and μ is the molecular dipole moment. The remaining terms have the same significance as in the Lennard-Jones potential.

Kihara Potential

The Kihara potential is an angle-dependent potential which was originally developed for spherocylindrical molecules (20). The potential has since been developed for a variety of differently shaped molecules. For spherical molecules with point centers the Kihara potential reduces to the Lennard-Jones potential. In the Kihara model each

core is surrounded by a penetrable soft shell which has a thickness ρ_0 . The potential energy is given by the following equation:

$$\psi(\rho) = \epsilon \left[(\rho_0/\rho)^{12} - 2(\rho_0/\rho)^6 \right] \quad (11)$$

where ρ is not the distance between centers (as r is in the Lennard-Jones potential) but is the distance between the surface of the impenetrable core of one molecule to that of the other. The distance between core surfaces depends upon the mutual orientation of the two molecules therefore making this an angle-dependent potential.

CHAPTER III

APPARATUS DESCRIPTION

Since this work was a continuation of previous work by the author, much of the apparatus used in this study has been previously described (21). There were some major changes in the design of the variable volume apparatus due to this previous experience. The major points which were considered in this new design were 1) the complete elimination of stopcocks from all points which could come in contact with the sample, 2) to minimize the surface to volume ratio by using spherical volumes, 3) to increase the total volume of the apparatus so that a larger sample could be used in making a run and 4) to facilitate cleaning.

Piezometer

The variable volume used in this study consisted of a glass piezometer made of eight spherical bulbs connected by two millimeter capillary tubing. The volumes of the bulbs were such that upon each compression step the pressure would increase by approximately one half of the initial pressure. The total volume of the piezometer was

318.82 milliliters. The volume calibration is discussed in Appendix A. A sketch of the apparatus is shown in Figure 2.

The upper most bulb was connected to the manometer by 2 millimeter capillary pyrex tubing. The manometer was constructed of 10 millimeter pyrex tubing. A reference mark on the sample side of the manometer was used as a constant height for the mercury level on that side. Etched reference marks were also placed on the capillary connecting the bulbs of the piezometer making possible the calibration of the piezometer bulb volumes. The piezometer and the manometer were connected with kovar seals through Hydromatic Series 715 ball valves D and E to respective mercury reservoirs. The connections of the metal tubing to the glass reservoirs were made with taped joints. A taped joint was made by placing a piece of aluminum foil over the joint made by butting the glass tube and metal tube together and then wrapping it with electrical tape. The joint was then painted with Sealit, allowed to dry, wrapped with more tape and again painted with Sealit. These joints were found to be satisfactory.

Sample Injection

The vacuum leg of the manometer was connected to the primary vacuum source and to the sample inlet apparatus. Hydromatic valves A and B were used to close off the

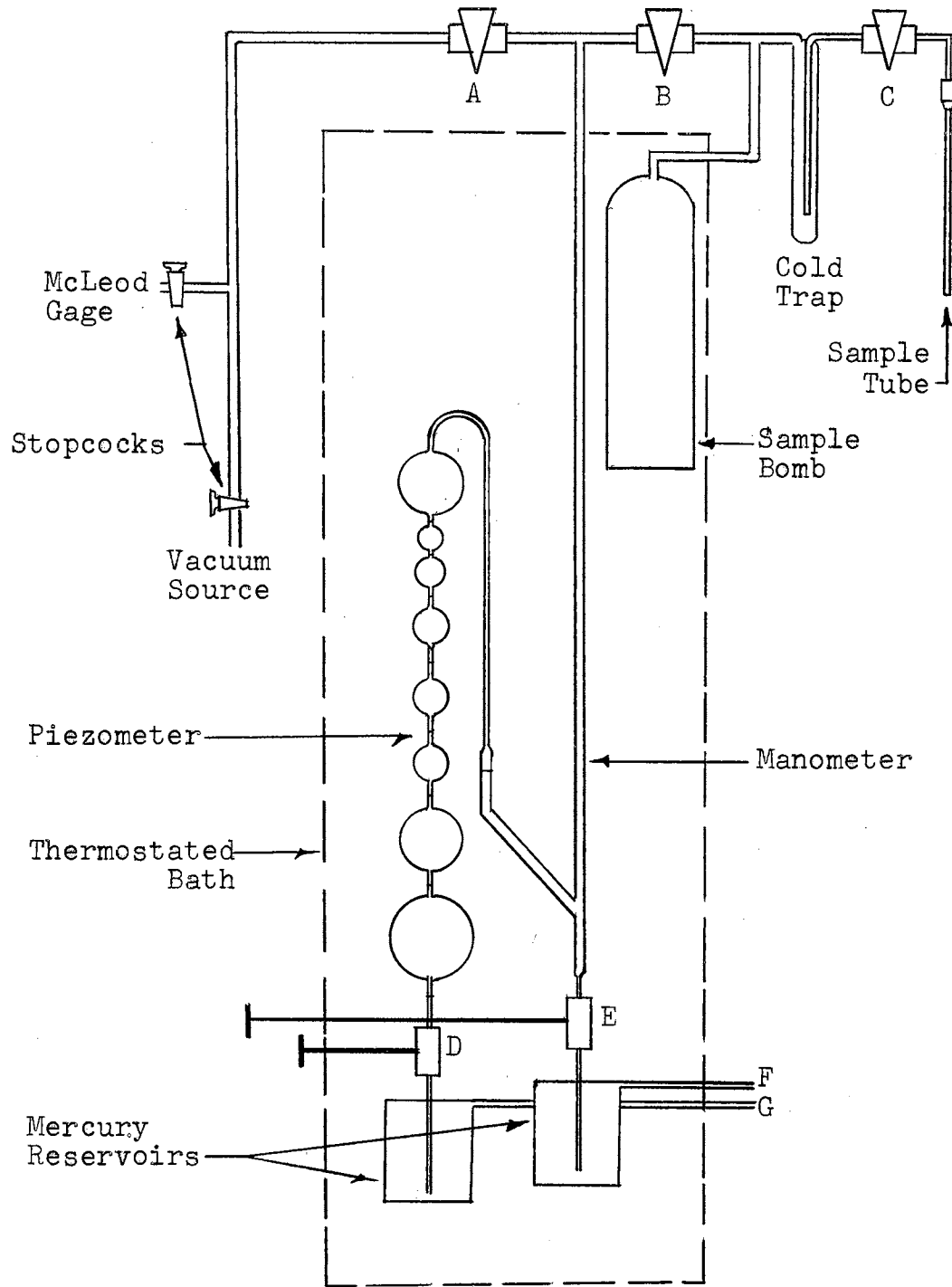


Figure 2. Low Pressure PVT Apparatus

manometer from the vacuum source and the sample inlet respectively.

The sample inlet was connected to a two liter glass sample bomb contained in the constant temperature bath. This bomb was connected to a cold trap which in turn was connected through a Hydromatic valve, C, to the sample tube. The sample tube was connected to the system by means of a 10/30 standard pyrex tapered ground glass joint. The sample tube was constructed of 2 millimeter pyrex capillary tubing with one end sealed and the male part of the ground glass joint on the other end. Kovar-to-glass seals were used with Swagelok fittings to make the connections with the metal ball valves.

The remainder of the apparatus including the constant temperature bath, primary vacuum source and other auxiliary equipment has been adequately described previously (21).

Materials

The benzene used in this work was Phillips research grade (99.98 mol %). The methyl alcohol was Baker reagent grade (99+ mol %, 0.05 % water and 0.001 % acetone impurities). The diethyl ether was Baker anhydrous reagent grade (99+ mol %, 0.01 % water and 0.01 % ethyl alcohol impurities). The acetone was Matheson spectroquality grade (99.9 mol %, 0.05 % water impurity). The ethyl

alcohol was pure grade. No attempt was made at further purification of these materials. All of the above materials were kept over Drierite or molecular sieve to keep the water content of these materials as low as possible. The diethyl ether was stored in a refrigerator to prevent evaporation.

CHAPTER IV

EXPERIMENTAL PROCEDURE

The initial procedure followed in preparing for a run has been adequately described previously (21). This includes the preliminary leak testing necessary before a run could be started and the procedure used to attain the desired temperature in the thermostated bath.

The procedure followed in making a run is described below. The first step was to inject a sample into the sample bomb. If the sample was to be a pure component, the pure material was put into the sample tube as a liquid. If the sample was to be a mixture, it was prepared by accurately weighing the components as liquids into the sample tube. A Mettler Model B5 balance was used to obtain these weights. The sample tube was then connected to the apparatus and a dewar containing liquid nitrogen was placed around it. A vacuum was applied to the frozen sample in the sample tube by opening valves A, B and C. The cold trap was then immersed in liquid nitrogen and the sample was allowed to distill into the cold trap where it was frozen out. Valves B and C were then closed. The liquid nitrogen was removed from the cold

trap and upon warming to room temperature the sample evaporated into the sample bomb. The sample pressure after makeup was usually 10 cm Hg or less and always well below the saturation pressure of the substances present. With a sample of this size, two or three runs could easily be made with the mixture or pure material originally placed in the sample bomb.

A run could be started after the sample had completely evaporated into the sample bomb. The piezometer was evacuated with the mercury just above valves D and E. After evacuation valve A was closed and valve B was opened. This charged the piezometer with a sample from the sample bomb. Valve B was then closed. The mercury in the manometer was raised to the reference mark on the sample side through valve E. Valve A was then opened. When the pressure on the vacuum side of the manometer was less than 5 microns mercury pressure, the mercury level in the piezometer was raised through valve D to the reference mark just below the bottom bulb. The mercury level in the sample side of the manometer was then readjusted to the reference mark using valve E. These mercury levels could be either raised or lowered by applying either a pressure or a vacuum through valves F and G to the mercury reservoirs.

After thermal equilibrium was reached (5 to 10 minutes), the mercury heights in both sides of the manometer

were measured with a cathetometer and recorded. Duplicate readings were taken with the cathetometer and if they differed by more than .005 cm a third reading was taken. The volume which the sample occupied is recorded as a volume number. These volume numbers refer to the calibrated volume nomenclature presented in Appendix A.

The lower most bulb was then filled with mercury until the mercury level was at the reference mark between the first and second bulb of the piezometer. The mercury level in the manometer was readjusted to the reference mark on the sample side. The quantities mentioned above were again measured and recorded after attaining thermal equilibrium. This procedure was followed compressing with mercury up through the lower seven bulbs and then expanding at least once to the lower most bulb. During the course of a run at least 10 datum points were taken, the last two of which were on expanding to check the reproducibility of the starting point of the run.

After completion of a run the mercury level in the manometer was lowered to just above valve E with Valve A closed. Valve A was then opened and the piezometer was evacuated in preparation for the next run. On several occasions the same sample was used to make a run at two different temperatures. In these cases after the first run was completed the bath temperature was raised or lowered to the desired point. The next run was started

after the bath temperature had attained steady state at the new temperature. Runs made in this fashion are designated A and B, for example Run 211A and Run 211B.

CHAPTER V

EXPERIMENTAL RESULTS

The experimental second virial coefficients derived for the pure substances and mixtures investigated in this study and the calculated interaction second virial coefficients are presented in this chapter. The calculational scheme used to obtain the second virial coefficients from the experimental data and a complete listing of the results for the individual tests are presented in Appendix B. The procedure used to obtain the interaction second virial coefficients is presented in Appendix C.

The temperature dependence of the second virial coefficients is shown in Figures 3, 4, 5 and 6 for benzene, methanol, ethanol, and acetone and diethyl ether respectively. The results obtained from this study are compared with existing data in these graphs. The lines included in the graphs are the estimated best representations of the experimental points.

The second virial coefficients obtained for binary mixtures of benzene-methanol, benzene-ethanol, benzene-acetone, and benzene-diethyl ether are tabulated with the calculated interaction coefficients in Tables I, II, III

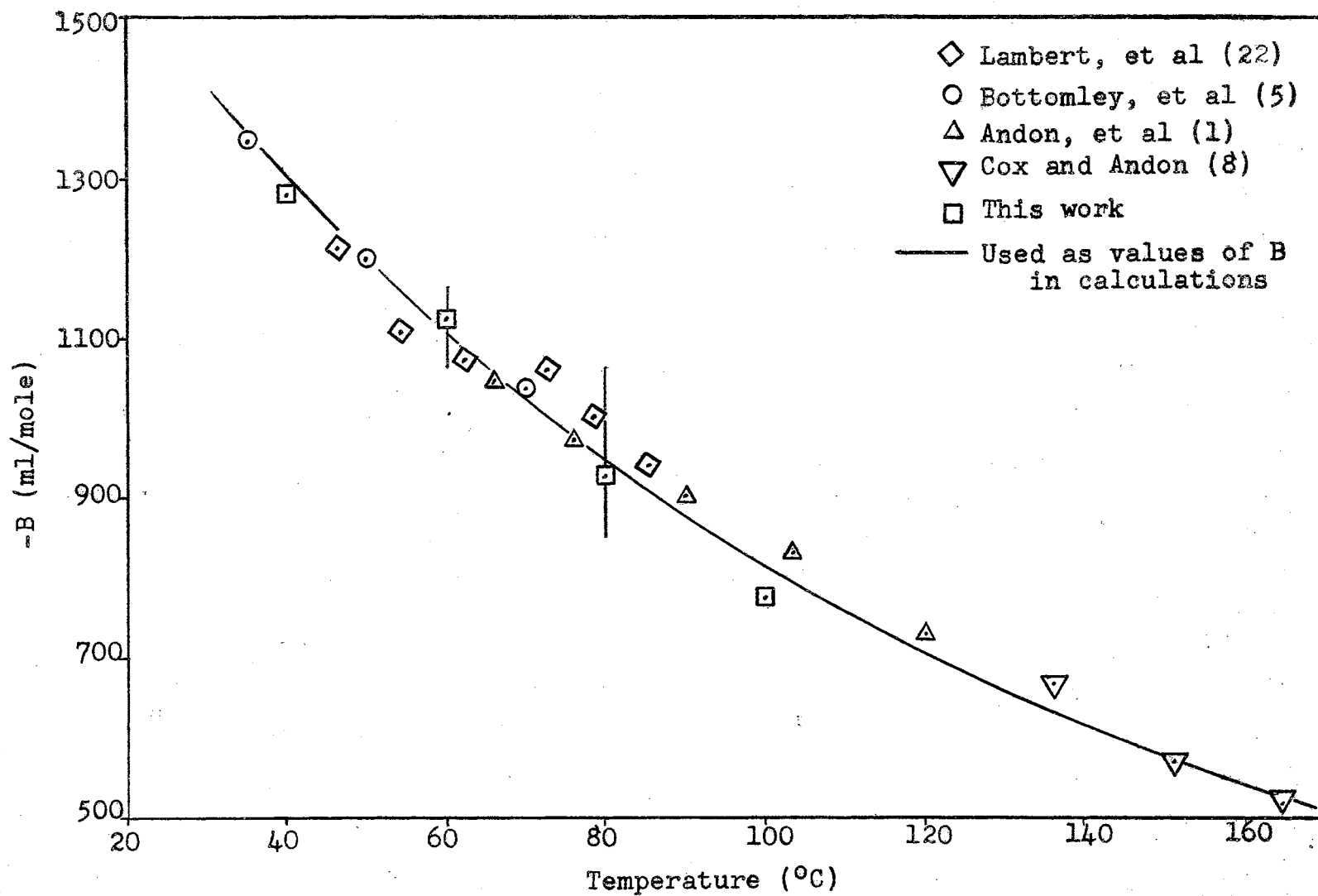


Figure 3. Second Virial Coefficient of Benzene Versus Temperature

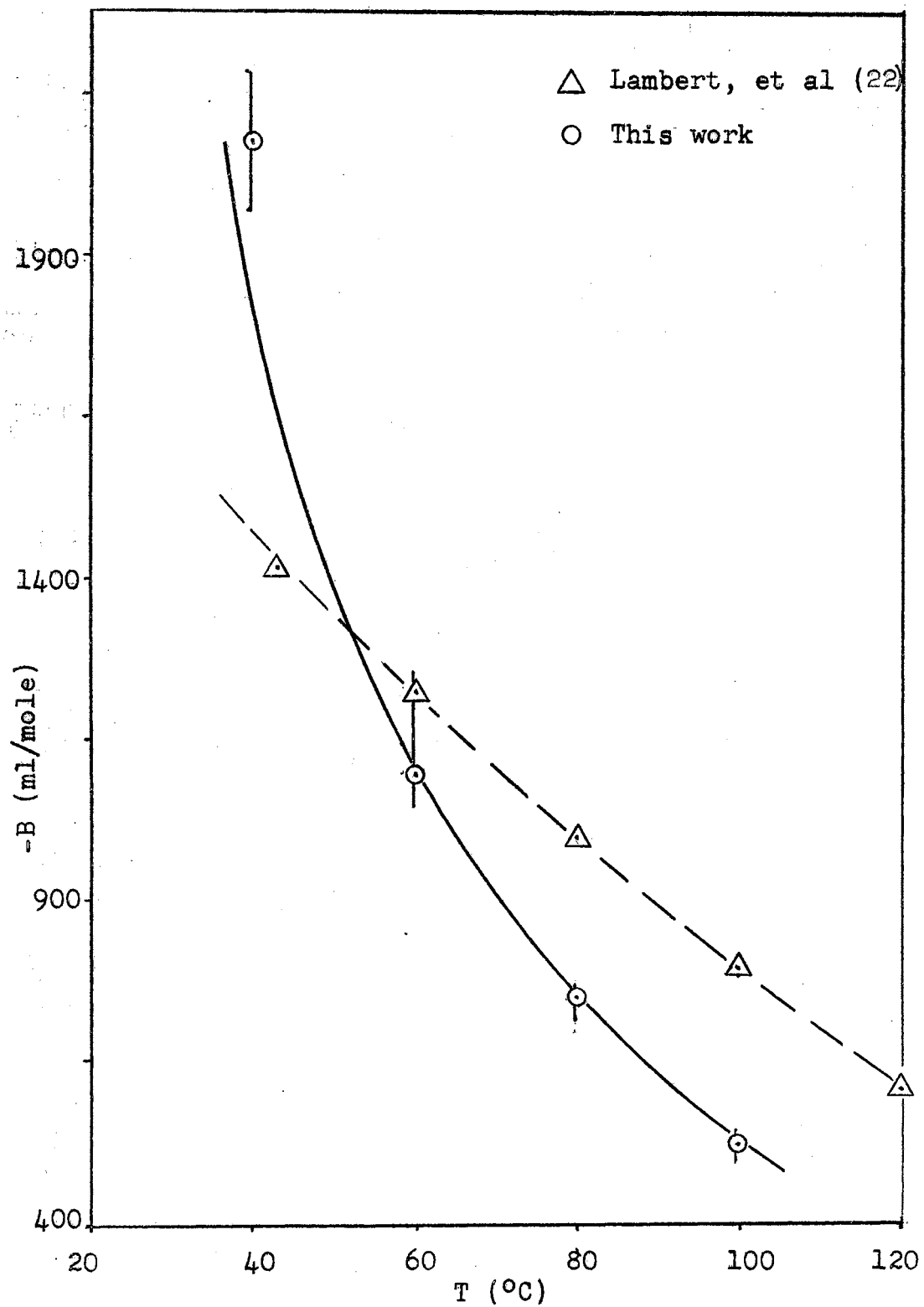


Figure 4. The Second Virial Coefficient of Methanol as a Function of Temperature

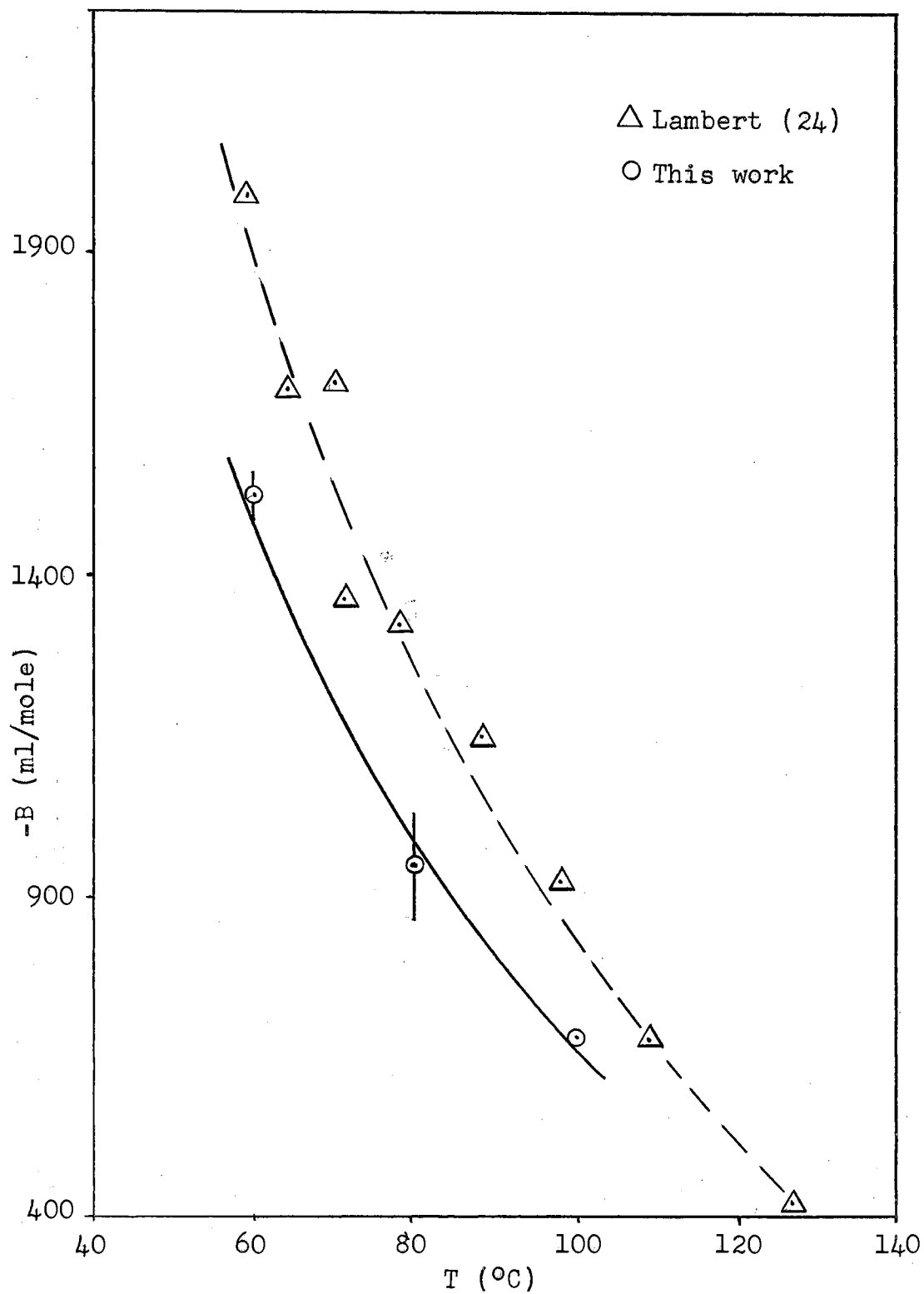


Figure 5. The Second Virial Coefficient of Ethanol as a Function of Temperature

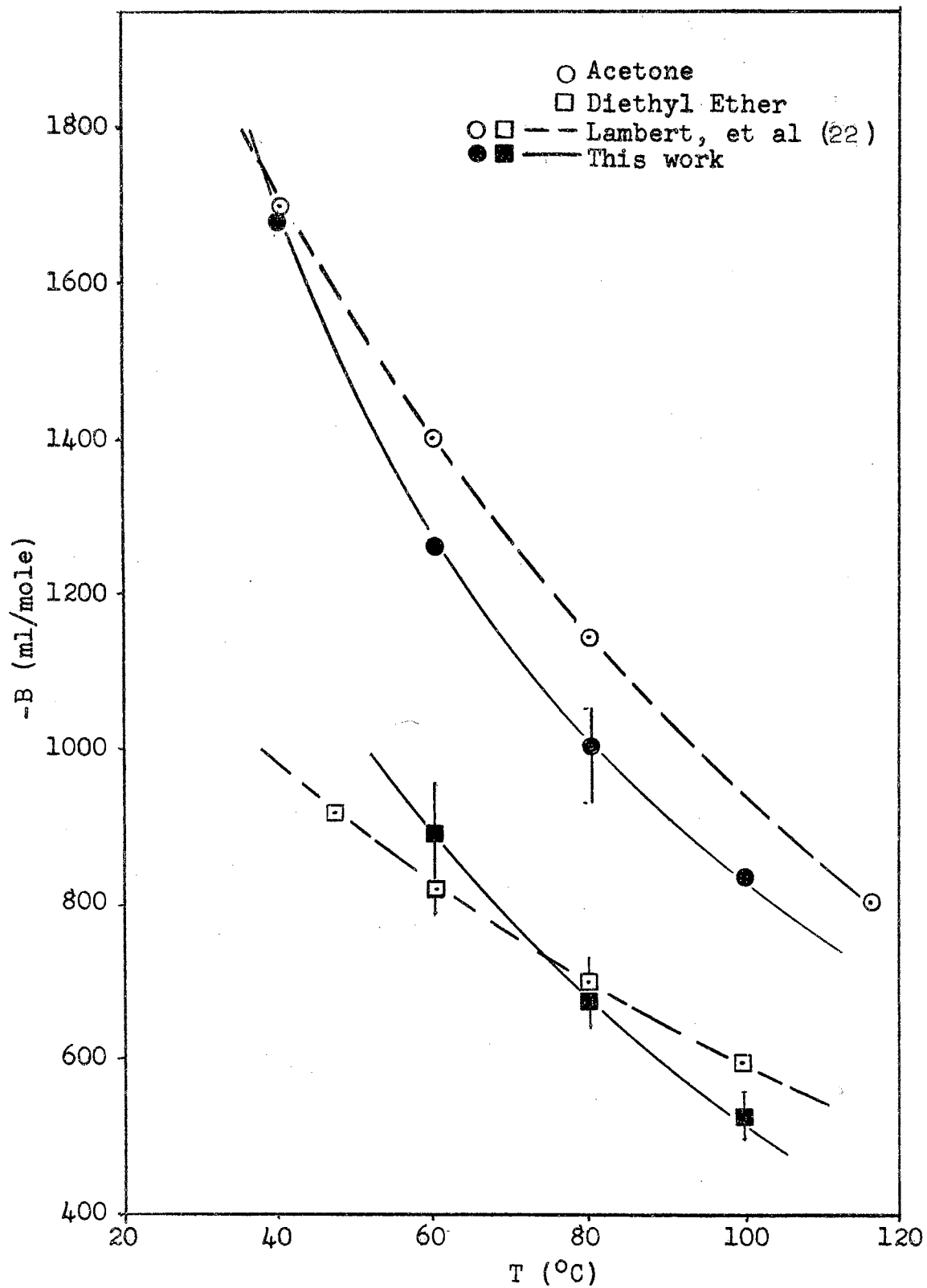


Figure 6. The Second Virial Coefficient of Acetone and Diethyl Ether as a Function of Temperature

TABLE I
 SUMMARY OF EXPERIMENTAL RESULTS
 BENZENE-METHANOL SYSTEMS

Temperature (°C)	Interaction Second Virial Coefficient (ml/mole)	Mole Fraction Benzene	Second Virial Coefficient (ml/mole)
40	-545	0.0000	-2079
		0.2039	-1522
		0.3147	-1314
		0.4749	-1099
		0.6379	-1091
		0.7717	-1134
		1.0000*	-1303
60	-507	0.0000	-1097
		0.2039	-970
		0.3147	-837
		0.4617	-775
		0.4749	-795
		0.6379	-838
		0.7239	-854
		0.7717	-882
1.0000*	-1107		
80	-319	0.0000	-752
		0.1843	-628
		0.2380	-601
		0.4349	-581
		0.5334	-588
		0.6521	-603
		0.6979	-649
		0.7239	-731
		1.0000*	-944
100	-281	0.0000	-524
		0.1903	-434
		0.4638	-478
		0.6961	-576
		1.0000*	-815

*These values are from Figure III.

TABLE II
 SUMMARY OF EXPERIMENTAL RESULTS
 BENZENE-ETHANOL SYSTEMS

Temperature (°C)	Interaction Second Virial Coefficient (ml/mole)	Mole Fraction Benzene	Second Virial Coefficient (ml/mole)
60	-567	0.0000	-1522
		0.2684	-1139
		0.4071	-979
		0.5712	-922
		0.7305	-913
		1.0000	-1107
80	-421	0.0000	-941
		0.2033	-759
		0.5168	-683
		0.7112	-742
		1.0000	-944
100	-490	0.0000	-687
		0.2071	-647
		0.5475	-629
		0.7067	-649
		1.0000	-815

TABLE III
 SUMMARY OF EXPERIMENTAL RESULTS
 BENZENE-ACETONE SYSTEMS

Temperature (°C)	Interaction Second Virial Coefficient (ml/mole)	Mole Fraction Benzene	Second Virial Coefficient (ml/mole)
40	-1376	0.0000	-1690
		0.2277	-1493
		0.4128	-1471
		0.5198	-1446
		0.7765	-1397
		1.0000	-1303
60	-930	0.0000	-1263
		0.2277	-1120
		0.4128	-1077
		0.5198	-1092
		0.7765	-1032
		1.0000	-1107
80	-698	0.0000	-1005
		0.2530	-912
		0.5301	-861
		0.6947	-815
		0.6991	-823
		1.0000	-944
100	-593	0.0000	-834
		0.2438	-752
		0.5019	-714
		0.7122	-709
		0.7405	-734
		1.0000	-815

TABLE IV
 SUMMARY OF EXPERIMENTAL RESULTS
 BENZENE-DIETHYL ETHER SYSTEMS

Temperature (°C)	Interaction Second Virial Coefficient (ml/mole)	Mole Fraction Benzene	Second Virial Coefficient (ml/mole)
60	-785	0.0000	-895
		0.2890	-865
		0.4124	-885
		0.5057	-885
		0.6800	-963
		0.7915	-979
		1.0000	-1107
80	-769	0.0000	-677
		0.2726	-734
		0.5365	-815
		0.7978	-860
		1.0000	-944
100	-620	0.0000	-525
		0.2461	-619
		0.5342	-651
		0.8052	-706
		1.0000	-815

and IV respectively. The results are plotted versus composition in Figures 7 through 10. The solid curves shown with the data in these plots were drawn using Equation 3 with the calculated interaction coefficients. The temperature dependence of the interaction coefficients is shown in Figure 11.

The results presented for the pure substances are the average values obtained from 2 to 8 tests at the same temperature. The results for the mixtures are either derived from a single test or the average value of duplicate tests. The vertical lines drawn through the data points in Figures 3 through 6 indicate the range of the results. The ends of the vertical lines through the data points in Figures 7 through 10 represent the individual values found for duplicate tests. If no line is shown the duplicate values fall within the designating symbol or only one test was made at that condition.

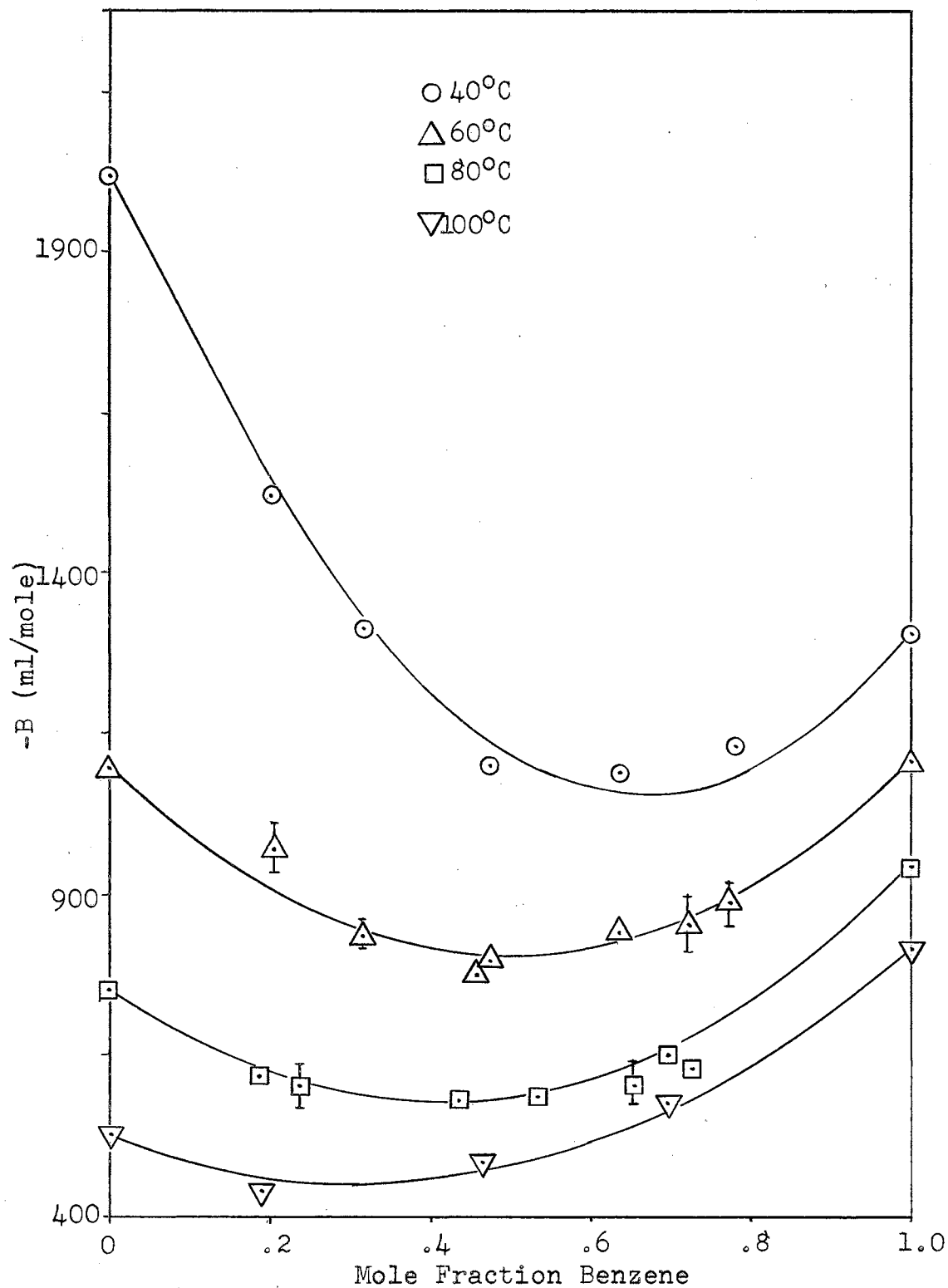


Figure 7. Second Virial Coefficients of the Benzene-Methanol System Versus Composition

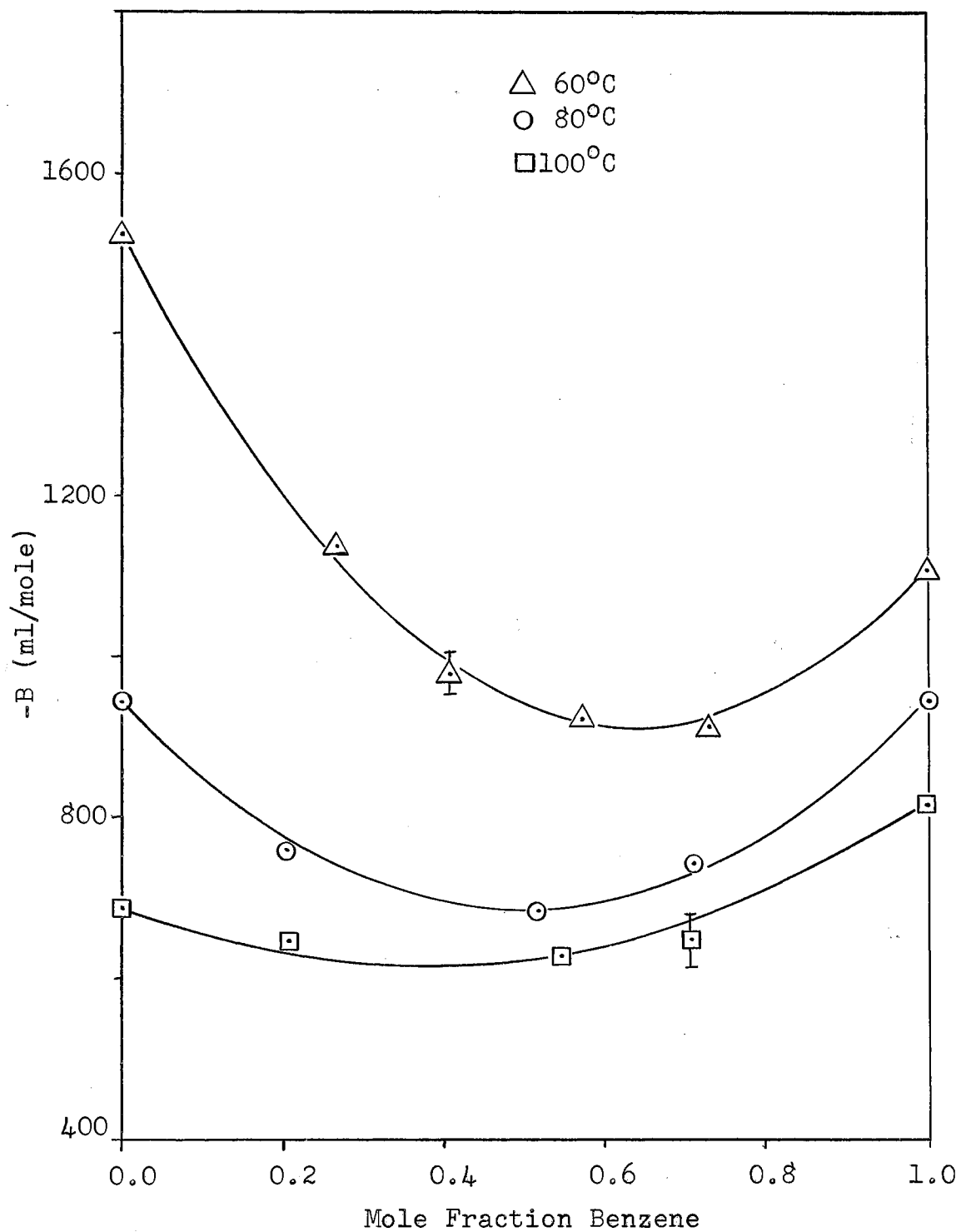


Figure 8. Second Virial Coefficients of the Benzene-Ethanol System Versus Composition

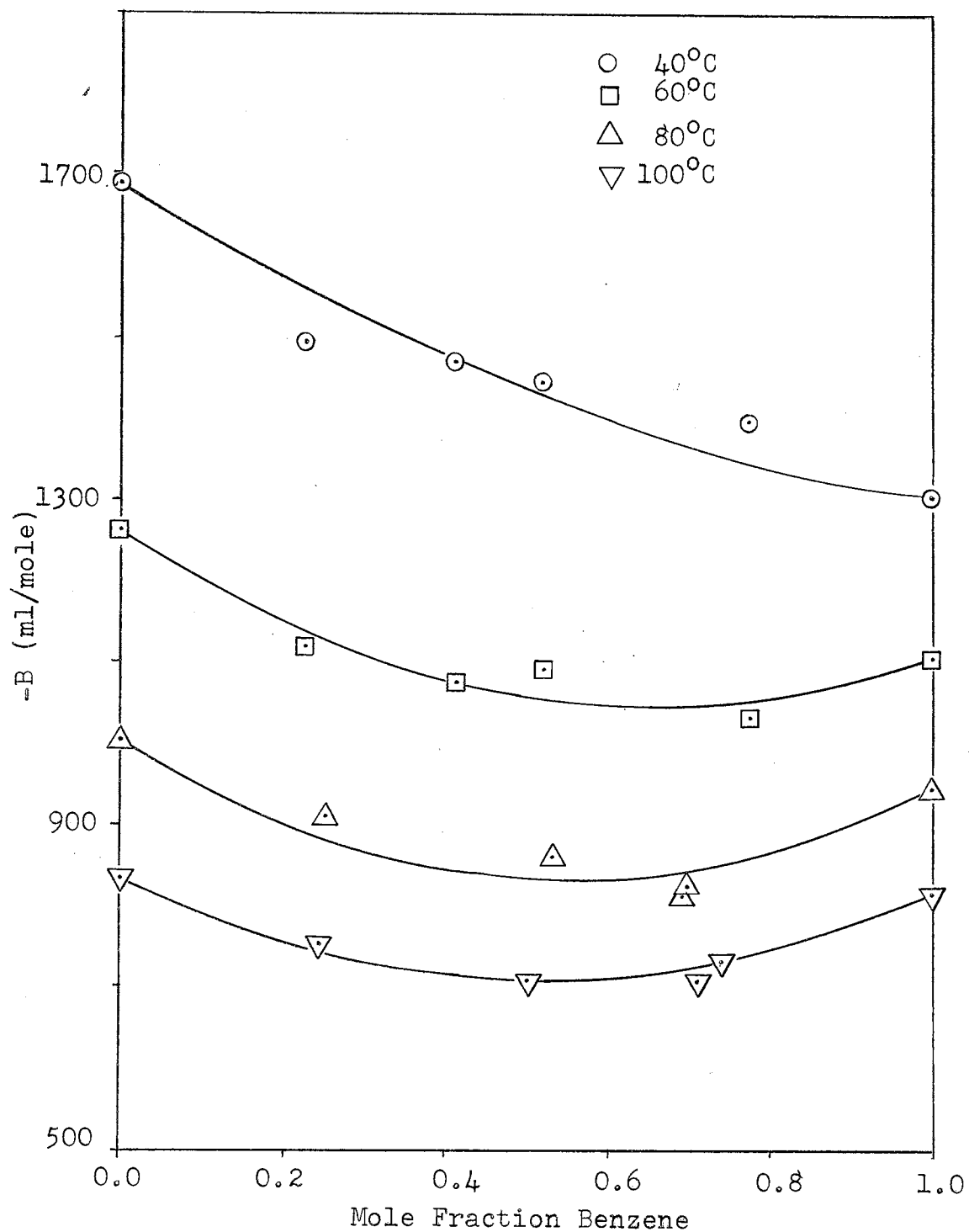


Figure 9. Second Virial Coefficients of the Benzene-Acetone System Versus Composition

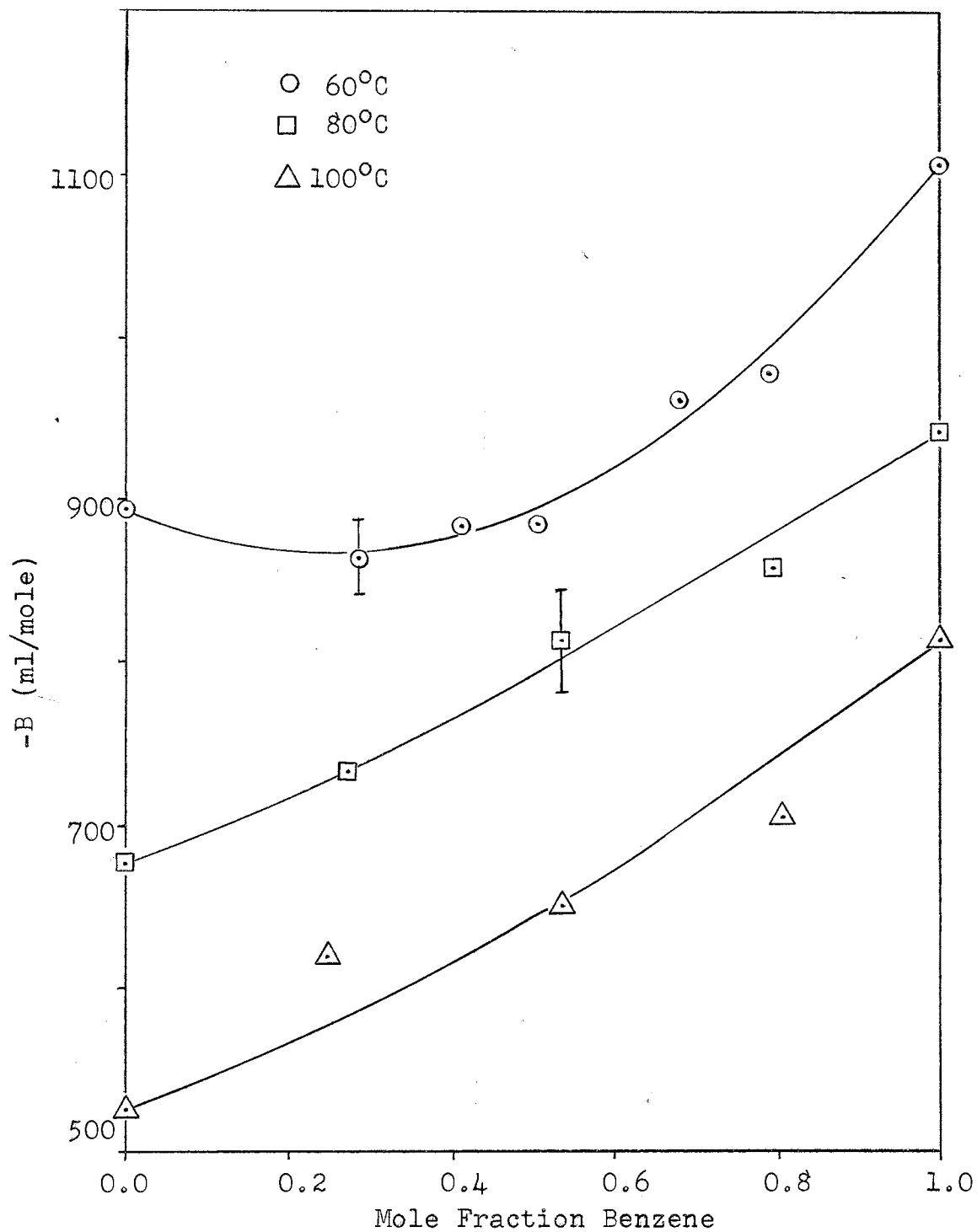


Figure 10. Second Virial Coefficients of the Benzene-Diethyl Ether System Versus Composition

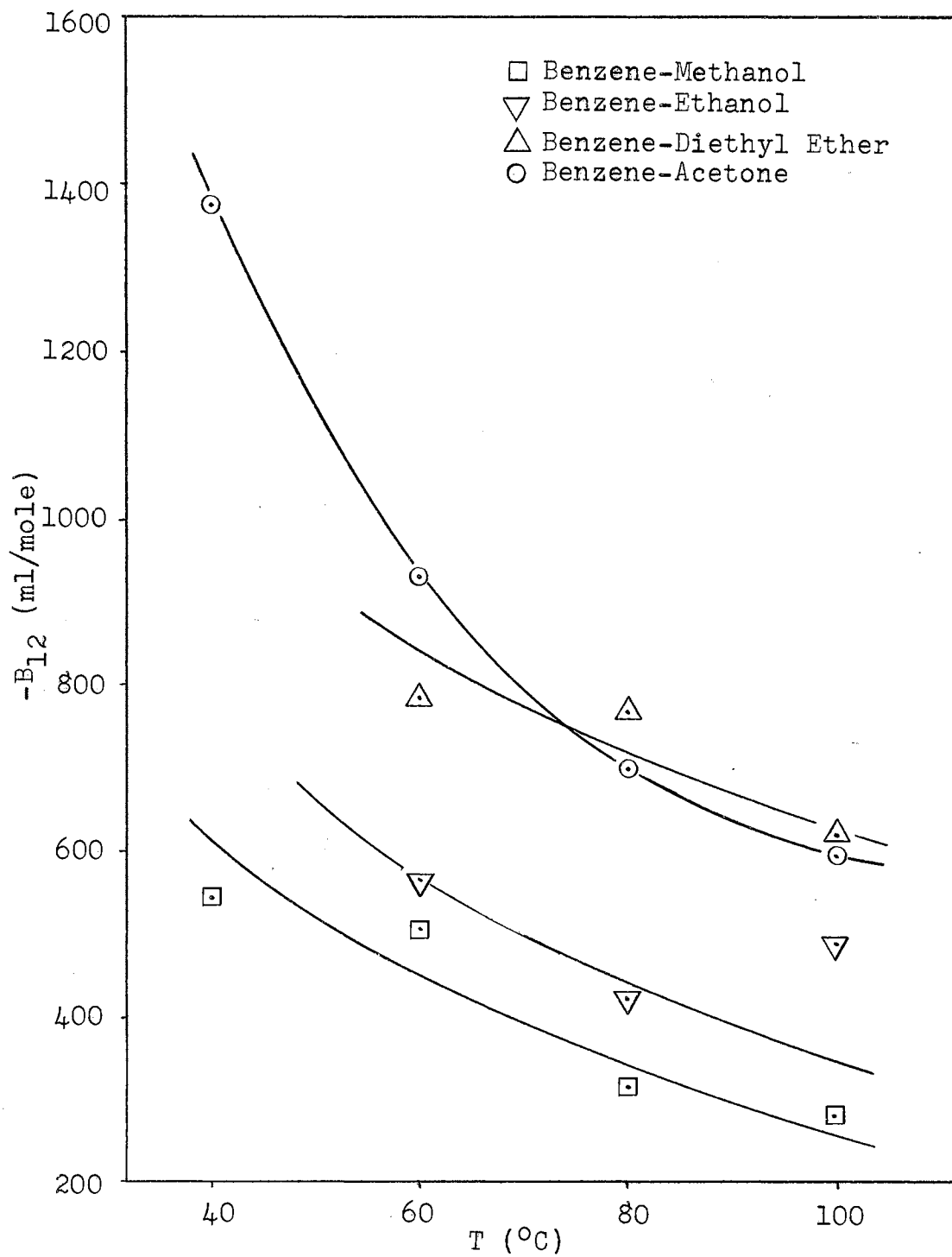


Figure 11. Temperature Dependence of the Interaction Second Virial Coefficients

CHAPTER VI

THEORETICAL TREATMENT OF RESULTS

In Chapter II several theoretical treatments of second virial coefficients are discussed. Certain of these treatments are here applied to the experimental results of this study. The potential functions are first fitted to the pure component results by determining the potential parameters. Next various methods of combining these parameters such that the interaction second virial coefficients can be calculated are discussed.

A nonlinear least squares procedure was used to determine the potential parameters by fitting the experimental second virial coefficients to the potential function. This procedure is discussed in Appendix E.

The Kihara potential parameters derived for the pure components studied in this work are presented in Table V. The parameters for benzene were determined using the results of this work and selected literature data presented in Figure 3. Also included in this table are the Kihara parameters determined from the available literature data for ethane, propane, isobutane and pentane. These parameters are used in a treatment of the interaction second

TABLE V
PARAMETERS FOR THE KIHARA POTENTIAL

	ρ_0 (Å)	a (Å)	ϵ/k (°K)	Std Dev (ml/mole)	Temperature Range (°C)
Benzene	3.370	0.00	1167.2	12.4	40-340
Ethane	2.472	0.00	729.4	8.2	35-238
Propane	5.940	0.00	256.81	1.9	35-238
Isobutane	5.890	0.00	325.1	5.6	35-238
Pentane	3.492	0.00	1046.2	2.7	35-238
Methanol	0.388	3.00	1724.7	26.1	50-100
Ethanol	0.331	3.20	1840.2	34.5	60-100
Acetone	2.166	0.20	1638.4	13.8	40-100
Diethyl Ether	1.407	0.20	1940.2	7.7	60-100

virial coefficients which is discussed later. The parameters presented for benzene, ethane, propane, isobutane and pentane are actually the Lennard-Jones parameters since the size of the impenetrable core, a , of the Kihara potential was set equal to zero. The parameter σ of the Lennard-Jones potential is equal to $2^{1/6}\rho_0$ when a point core ($a = 0$) is used with the Kihara potential.

The experimental data for methanol, ethanol, acetone and diethyl ether were fitted with the Kihara potential using spherical impenetrable cores. The size of the impenetrable core, a , was varied so as to obtain the best fit of these data. The criterion used to determine the best fit was the minimum value of the standard deviation.

The Stockmayer potential was also used to fit the data of methanol, ethanol, acetone and diethyl ether. The problems of determining the Stockmayer parameters by a non-linear least squares procedure are compounded due to the presence of the third parameter, t^* . This parameter changes with both ϵ/k and σ which causes some problems in obtaining convergence. The parameters obtained for this model are presented in Table VI.

Interaction Second Virial Coefficients

The theoretical interaction second virial coefficients were calculated using several different procedures. The parameters determined for the methods using the potential functions are presented in Table VII. The results of the

TABLE VI
STOCKMAYER PARAMETERS

	ϵ/k ($^{\circ}\text{K}$)	σ (\AA)	t^*	Std Dev (ml/mole)
Methanol	762	2.54	.565	140.0
Ethanol	624.2	2.44	.804	14.1
Acetone	506.2	3.77	.709	50.0
Diethyl Ether	1112.8	2.39	.228	32.5

TABLE VII
MIXTURE POTENTIAL PARAMETERS

Kihara Potential

	$(\rho_0)_{12}$ (\AA)	$(\epsilon/k)_{12}$ ($^{\circ}\text{K}$)	$\frac{a_1}{\text{\AA}}$	$\frac{a_2}{\text{\AA}}$
Benzene-Methanol	1.879	1419.8	0.00	3.00
Benzene-Ethanol	1.850	1465.0	0.00	3.20
Benzene-Acetone	2.768	1382.9	0.00	0.20
Benzene-Diethyl Ether	2.388	1504.9	0.00	0.20

Lennard-Jones Potential (Using Stockmayer parameters for polar components)

	$(\rho_0)_{12}$ (\AA)	$(\epsilon/k)_{12}$ ($^{\circ}\text{K}$)
Benzene-Methanol	3.115	943
Benzene-Ethanol	3.06	854
Benzene-Acetone	3.81	769
Benzene-Diethyl Ether	2.98	1128

Lennard-Jones Potential (Using homomorph parameters for polar components)

	$(\rho_0)_{12}$ (\AA)	$(\epsilon/K)_{12}$ ($^{\circ}\text{K}$)
Benzene-Methanol	2.920	922.7
Benzene-Ethanol	4.655	547.6
Benzene-Acetone	4.630	616.0
Benzene-Diethyl Ether	3.430	1104.9

Lennard-Jones Potential (Using homomorph parameters for polar components and accounting for dipole-induced dipole effects)

	$(\rho_0)_{12}$ (\AA)	$(\epsilon/k)_{12}$ ($^{\circ}\text{K}$)	α_1 (cm^{-3})	μ_2 (debyes)
Benzene-Methanol	2.896	1018.2	10.32	1.66
Benzene-Ethanol	4.651	553.5	10.32	1.69
Benzene-Acetone	4.620	632.1	10.32	2.74
Benzene-Diethyl Ether	3.425	1122.3	10.32	1.16

interaction second virial coefficient determinations are presented in Table VIII with the values derived from the experimental data.

The first procedure to be discussed used the classical mixing rules (13) given by the following equations:

$$T_{c12} = (T_{c11}T_{c22})^{\frac{1}{2}} \quad (11)$$

$$P_{c12} = (P_{c11}P_{c22})^{\frac{1}{2}} \quad (12)$$

The Berthelot equation of state was used with the above equations to determine the interaction second virial coefficients.

The Stockmayer parameters derived for the polar materials were used with the Lennard-Jones parameters for benzene to determine the mixture parameters given by the following equations:

$$(\epsilon/k)_{12} = [(\epsilon/k)_{11} (\epsilon/k)_{22}]^{\frac{1}{2}} \quad (13)$$

$$\sigma_{12} = (\sigma_{11} + \sigma_{22})/2 \quad (14)$$

Using these mixture parameters in the Lennard-Jones potential the interaction second virial coefficients were calculated. These results are listed under the Stockmayer heading in Table VIII.

In applying the Kihara potential to mixtures with $a = 0$ for one component (benzene in the mixtures considered here) the following equation is obtained:

TABLE VIII

INTERACTION SECOND VIRIAL COEFFICIENTS

Mixture	Temperature (°C)	Experiment	Berthelot (milliliters/gram mole)	Lennard-Jones	Kihara	Using (4)	Homomorphs (5)
Benzene-Methanol	40.00	-545	-841	-576	-2563	-449	-565
	60.00	-507	-738	-495	-1998	-387	-480
	80.00	-319	-651	-431	-1598	-338	-415
	100.00	-281	-581	-381	-1304	-299	-364
Benzene-Ethanol	60.00	-567	-825	-372	-2375	-544	-553
	80.00	-421	-728	-328	-1884	-490	-498
	100.00	-490	-642	-292	-1527	-444	-452
Benzene-Acetone	40.00	-1376	-1072	-654	-1457	-747	-781
	60.00	-930	-941	-573	-1170	-665	-693
	80.00	-698	-833	-509	-963	-596	-621
	100.00	-593	-735	-456	-810	-539	-561
Benzene-Diethyl Ether	60.00	-785	-951	-685	-1039	-990	-1029
	80.00	-769	-837	-584	-839	-847	-879
	100.00	-620	-738	-507	-695	-737	-763

(4) Parameters of homomorphs used in calculation of interaction parameters. Lennard-Jones potential used to calculate the interaction second virial coefficients.

(5) Same as (4) except that correction is made for the dipole-induced dipole interaction.

$$\begin{aligned}
 B_{12} = & 2/3 N (\rho_0)_{12}^3 F_1 + \frac{M_{02} (\rho_0)_{12}^2}{2} F_2 \\
 & + \frac{S_{02} (\rho_0)_{12}}{2} F_3 + \frac{V_{02}}{2}
 \end{aligned}
 \tag{15}$$

The parameters $(\rho_0)_{12}$ and $(\epsilon/k)_{12}$ are calculated using Equations 13 and 14. The results of these calculations are presented under the Kihara heading in Table VIII.

The fourth method considered here assumes the interaction between the nonpolar molecules and polar molecules to be the same as that between the nonpolar molecules and nonpolar molecules of approximately the same size and shape as the polar molecules. The molecules used to represent the polar molecules in this fashion are called homomorphs. The homomorphs for methanol, ethanol, acetone and diethyl ether were chosen to be ethane, propane, isobutane and pentane respectively. The Lennard-Jones parameters for these molecules are used with Equations 13 and 14 to obtain the interaction parameters. These parameters were then used in the Lennard-Jones potential to calculate the interaction second virial coefficients listed in Table VIII under heading number 4.

The final method used to calculate the interaction second virial coefficients uses the parameters of the homomorphs as the nonpolar parameters of the polar materials but assumes there is a dipole-induced dipole effect which must be accounted for in the interaction of polar with nonpolar molecules. This dipole effect can be calculated using the

equation (3):

$$\xi_{12} = \frac{\alpha_1 \mu_2^2}{4 \left(\frac{\sigma_{11} + \sigma_{22}}{2} \right)^6 (\epsilon_{11} \epsilon_{22})^{\frac{1}{2}}} \quad (16)$$

where α_1 is the polarizability of the nonpolar molecule, μ_2 is the dipole moment of the polar molecule. The effects of this quantity on the interaction potential parameters σ_{12} and $(\epsilon/k)_{12}$ are given by the following equations:

$$\sigma'_{12} = \frac{1}{2}(\sigma_{11} + \sigma_{22})(1 + \xi_{12})^{-1/6} \quad (17)$$

$$(\epsilon/k)'_{12} = \left[(\epsilon/k)_{11} (\epsilon/k)_{22} \right]^{\frac{1}{2}} (1 + \xi_{12})^2 \quad (18)$$

These modified parameters are used in the Lennard-Jones potential to calculate the interaction second virial coefficients. The results of these calculations are presented in Table VIII under heading 5.

CHAPTER VII

DISCUSSION OF RESULTS

The discussion of results is divided into two sections. The first section is concerned with the experimental results and the second concerns the results obtained from applying the available theories to the experimental results.

Experimental Results

The author's first attempt at obtaining second virial coefficients from low pressure PVT data resulted in failure (21). This was due to the presence of distinct curvature in plots of PV versus P from which the second virial coefficients are derived. It was suspected that this curvature was caused by the adsorption of the sample vapor by foreign material in the system. This problem arose several times during the experimental investigation of this study but was always corrected by thorough cleaning of the apparatus. This behavior was noted in Runs 262, 263, 264 and in the runs made after Run 386. The results of these runs are not included in the complete tabulation of results given in Appendix B. Figure 12 shows a typical linear relation

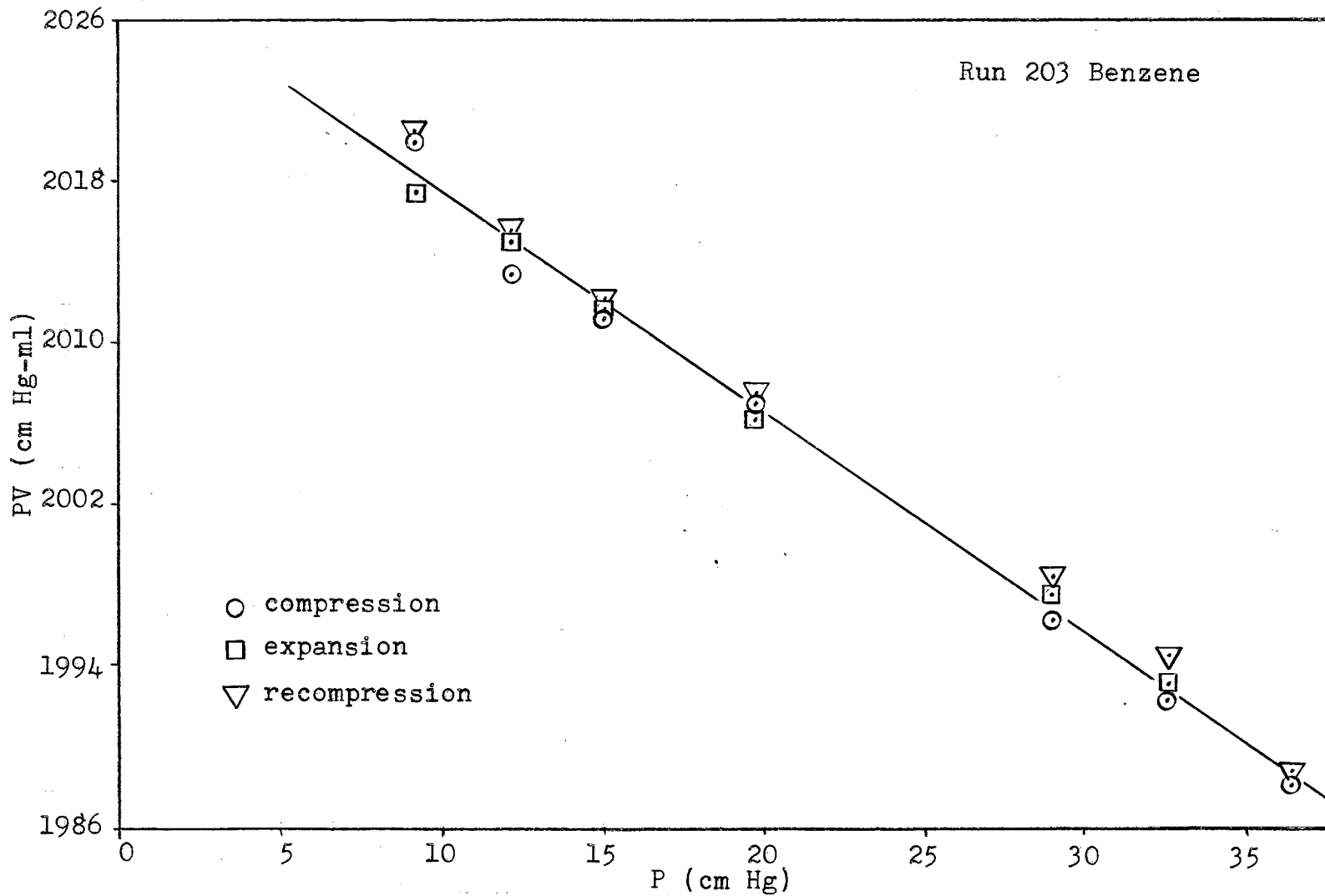


Figure 12. Typical Plot of PV versus P

between PV and P from which the derived second virial coefficient is consistent with the accuracy expected from the apparatus. In Figure 13 the curvature in the relationship between PV and P discussed above is present.

The data obtained at 40°C in this study are not as accurate as the data obtained at the higher temperatures. This is due to inherent error in determining the pressure and the low pressures required to stay below the saturation vapor pressures at 40°C . The temperature dependence of the vapor pressures of the materials used in this study are shown in Figure 14. It is seen from this figure that the vapor pressure is especially restrictive for benzene and ethanol at the lower temperatures. The error in measuring the sample pressure at various pressures is thoroughly discussed in Appendix D.

Second virial coefficients are reported in Chapter V for the benzene-methanol and benzene-acetone systems at 40°C . However due to the increased error in the measurement of the data, these results should be regarded as qualitative rather than quantitative.

The second virial coefficients presented in Chapter V were calculated using Equation 2. For comparison, the second virial coefficients were also calculated using Equation 1. The difference between the calculated second virial coefficients using these two equations is less than the experimental error. The results obtained using

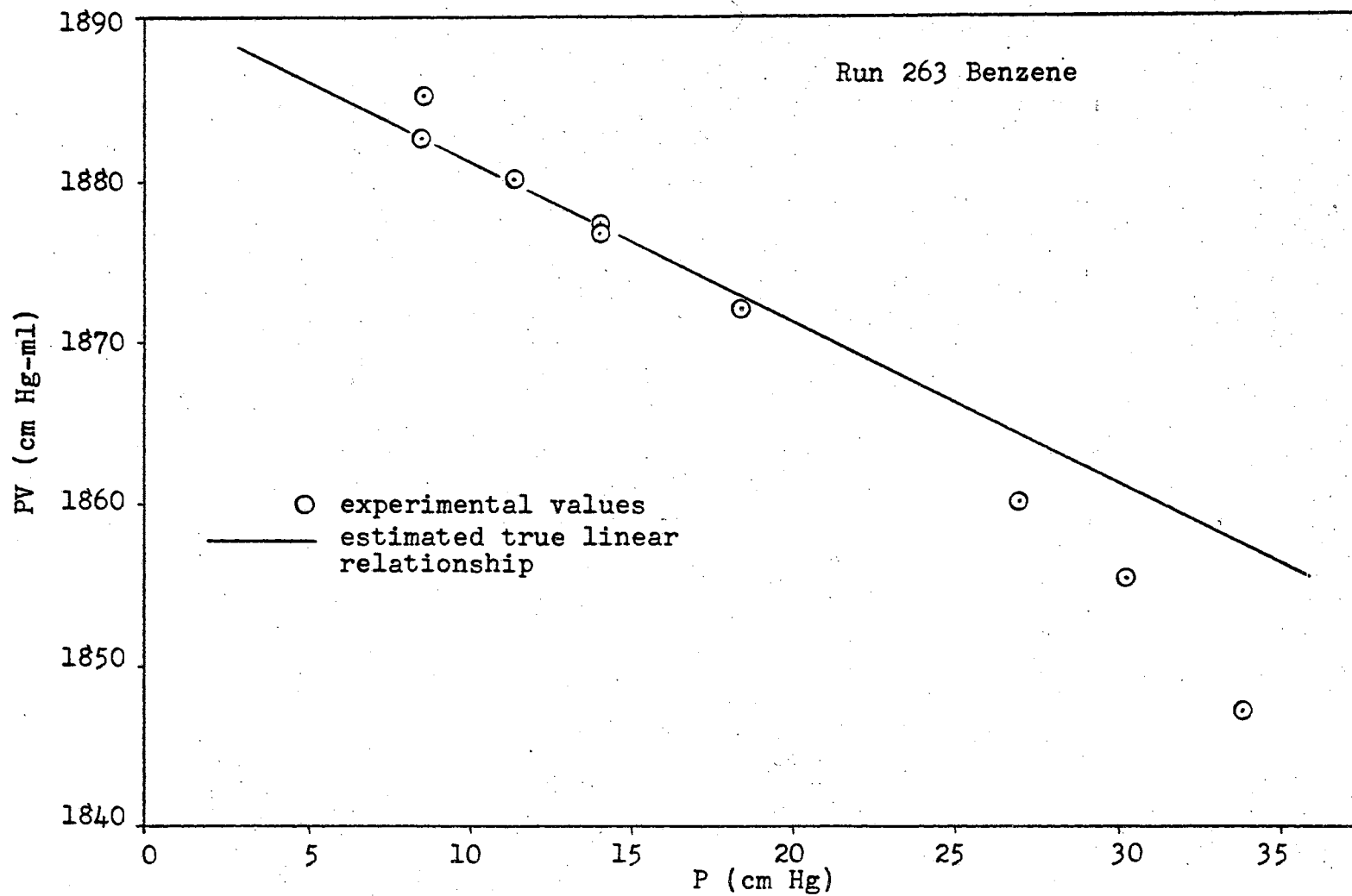


Figure 13. Behavior of PV versus P Relationship When Adsorption is Present

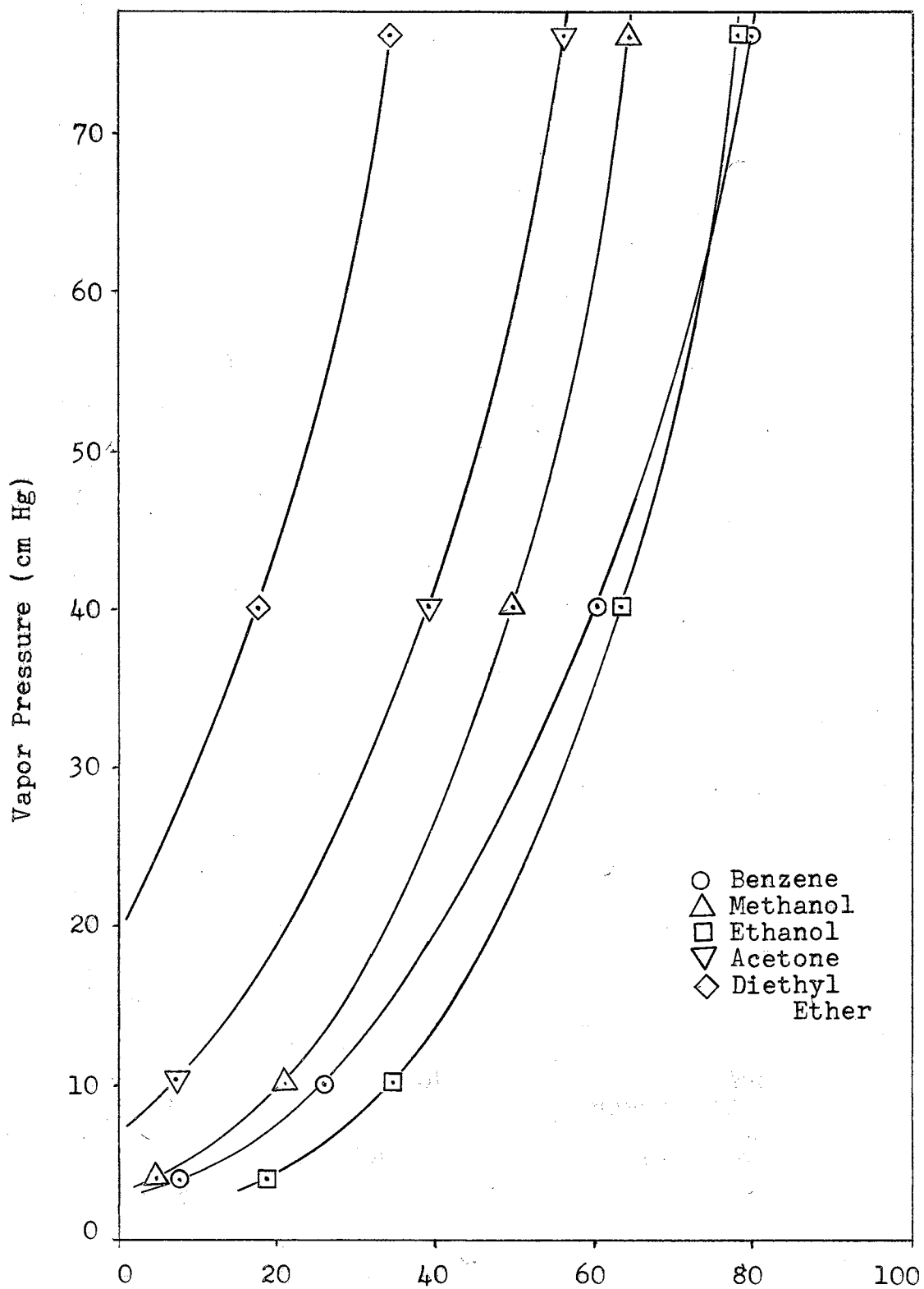


Figure 14. Vapor Pressure versus Temperature

Equation 1 are presented in Appendix B.

The experimental second virial coefficients for benzene obtained in this study are shown in Figure 3. These results agree within experimental error with the literature data. There is a large quantity of data reported in the literature for benzene. The values shown in Figure 3 are the most recent and the best available due to recent improvements in experimental techniques. The values used in the calculations were obtained from the best line fit through these data as shown. Lambert's data (22) for benzene are shown for comparison since the only literature data available for methanol, ethanol, acetone and diethyl ether are those presented by Lambert. As seen in Figure 4, 5, and 6 the results obtained in this work for these materials have a greater temperature dependence than the results presented by Lambert. The absolute values of the second virial coefficients obtained in this study also tend to be lower at the higher temperatures.

The data for acetone at 40 and 60°C were obtained using the same vapor sample. The quantities of vapor calculated to be in the piezometer for each of these runs are in excellent agreement. These results are tabulated in Table D-IV in Appendix D. The duplicate values found at each temperature also agree quite closely. It is therefore felt that the acetone data obtained in this work are especially good. The methanol, ethanol and diethyl

ether results are acceptable although the deviation from Lambert's results cannot be explained.

The mixture data shown in Figures 7 through 10 when observed from the aspect of precision are very good. These figures also show that the curves calculated using the derived interaction coefficients are in excellent agreement with the experimental results. To this point in the analysis it would seem that the mixture data are very good. However when the interaction coefficients are plotted versus temperature, a great deal of scatter is present as shown in Figure 11. The interaction coefficients for the benzene-methanol and benzene-acetone systems follow more nearly the expected behavior than do those of the benzene-ethanol and benzene-diethyl ether systems.

In Appendix D the calculated deviation of the pure component experimental second virial coefficients from the arithmetic average values was found to be ± 29.4 ml/mole. The average deviation of the duplicate results obtained for each mixture was ± 13.4 ml/mole. A part of this difference can be explained in that several liquid samples were used in obtaining the pure component data whereas the same liquid sample was used for the duplicate mixture data. The average standard deviation calculated from the statistical analysis of the PV versus P data for each run was found to be ± 32.1 ml/mole. The standard deviations calculated for each run are tabulated in Appendix D. It

should be noted that in discussing the precision of the data, the absolute value of the second virial coefficient is not important. If the second virial coefficient is equal to 100 ml/mole, the precision would be the same as when it is equal to 1500 ml/mole, i.e., ± 32.1 ml/mole. This is due to the manner in which the second virial coefficients are calculated, specifically from a plot of PV versus P. The precision of the PV and P measurement is the same regardless of the value of the derived second virial coefficient.

In the determination of the interaction coefficients, three experimentally determined second virial coefficients are used. These are B_M , B_{11} and B_{22} . If the error in each of these is ± 32.1 ml/mole the expected deviation in B_{12} would be approximately ± 100 ml/mole excluding any error in the composition of the mixture. This large expected deviation explains the uncertainties observed in the values of the interaction second virial coefficients. The error associated with the determination of the binary compositions was less than 0.2%. This accounts for the errors in weighing the components together. There is also the possibility that the composition was slightly affected when the mixture was injected into the apparatus. Several of these mixtures were analyzed on a gas chromatograph in the presence of argon but the chromatogram proved to be less accurate than the weighings used to make up the

mixtures. Therefore the results of these tests were inconclusive.

Theoretical Treatments

The association theory of Lambert (22) is briefly mentioned in Chapter II. Although no results are presented in Chapter VI, some preliminary calculations were made using this treatment. From these calculations some insight can be gained into the nature of the association between molecules. The results for ΔH and ΔS of Equation 5 were similar to those obtained previously (27). Rowlinson has thoroughly discussed these results (32). Since interaction second virial coefficients cannot be calculated a priori using this approach no further calculations were made.

In Table V it is seen that the Lennard-Jones potential was fit to the benzene second virial coefficients with a standard deviation of 12.4 ml/mole over a temperature range of 40 to 340°C. This deviation is well within the experimental error. Sherwood and Prausnitz (34) in fitting the Lennard-Jones potential to benzene found a standard deviation of 39.5 ml/mole. In applying the Kihara potential to benzene these authors were able to obtain a fit with a standard deviation of 5.6 ml/mole. The difference in the standard deviations found in using Lennard-Jones potential can be accounted for by the fact that Sherwood and Prausnitz used 30 experimental data points

whereas in this study 10 average values were used covering the indicated temperature range.

The experimental data used to obtain the Lennard-Jones parameters for ethane, propane, isobutane and pentane covered a temperature range of 35 to 238°C. The standard deviations presented in Table V for these fits show that the Lennard-Jones potential adequately represents the second virial coefficients of these compounds as was expected.

The Kihara potential was found to adequately describe the second virial coefficients of methanol, ethanol, acetone and diethyl ether obtained in this study. Since the data ranged from 40 to 100°C for methanol and acetone and from 60 to 100°C for ethanol and diethyl ether, the parameters determined are adequate to fit the experimental data within the experimental error. However it should be noted that any potential could be used over such a limited temperature range with similar success.

The parameters of the Stockmayer potential were determined for methanol, ethanol, acetone and diethyl ether. The Stockmayer potential was found to fit only the second virial coefficients of ethanol better than the Kihara potential. In order to fit the Stockmayer potential to the data of methanol, the tabulated potential values had to be extrapolated to cover a wider range of variables. If this potential is to be used extensively for polar

compounds, the tabulated values of the potential will have to be first extended to cover the entire range of variables of interest.

As previously mentioned, in applying the potential functions to the second virial coefficients obtained in this study the validity of the determined parameters is limited by the small temperature range of the results. The one exception is benzene where a vast quantity of data are available in the literature. If the determined pure component potential parameters are used to calculate the potential parameters necessary for the determination of the interaction coefficients, the uncertainty in these results is expected to be quite large. Since the experimental uncertainty in the determined interaction second virial coefficients is ± 100 ml/mole, the best one can expect from applying theoretical considerations is an idea of which method would be of greater use in calculating these coefficients if no experimental data were available.

The results shown in Table VIII illustrate that of the approaches applied here, the use of homomorphs to represent the polar parameters was the most successful for the benzene-methanol and the benzene-ethanol systems. The most adequate treatment of the benzene-acetone system was obtained using the Kihara potential. In the case of the benzene-diethyl ether system all treatments applied gave approximately the same results.

The approach using homomorphs to obtain the approximate nonpolar potential parameters of the polar molecules has been used by Blanks and Prausnitz (3). However even after the correction was made for dipole-induced dipole interactions to obtain agreement with experimental values, it was necessary to multiply the correction factor given by Equation 17 by an additional constant. This constant ranged from 10 to 70 and was a function of the difference between $\sigma_{\text{Stockmayer}}$ and σ_{nonpolar} . The latter being given by the homomorph. The application of this additional constant was not necessary in applying this approach to the results of this study.

When the Berthelot equation of state was used to calculate the second virial coefficients of the pure compounds used in this study, rms deviations of 36.9, 830, 565, 442 and 81.7 ml/mole were found for benzene, methanol, ethanol, acetone and diethyl ether respectively. It can be seen from these deviations that this equation of state can be used with success with benzene and with increasing success with polar compounds as the dipole moves toward the center of the molecule. The Berthelot equation underestimates the interaction of like polar molecules in that the absolute magnitude of the second virial coefficients is too small. However, as shown in Table VIII, when the Berthelot equation is applied to the mixtures studied the interaction between unlike molecules is overestimated.

This is good proof that the interactions between the non-polar and polar molecules of this study are similar to the interaction between like or unlike nonpolar molecules. The overestimation of the interaction between the unlike molecules of the mixtures can be explained by the fact that the critical constants of polar molecules are influenced by the presence of the dipoles.

The excellent agreement obtained for the benzene-methanol and benzene-ethanol systems using the homomorph parameters as the nonpolar parameters also indicates that the interactions between the polar and nonpolar molecules investigated in this study are similar to the interactions of nonpolar molecules.

CHAPTER VIII

CONCLUSIONS AND RECOMMENDATIONS

A great portion of this study was devoted to modifying a low pressure, variable volume PVT apparatus (21) and collecting PVT data for 4 binary mixtures of benzene and a polar component. The theoretical treatment consisted of finding a calculational method and proposed mixing rules which would be applicable, if any, to the type of systems considered in this study.

The main conclusions which can be drawn from this study are:

- 1) The modified experimental apparatus used in this study is adequate to provide PVT data for binary mixtures and pure component vapors over the temperature range of 60 to 100 °C.
- 2) The accuracy of the experimental data compares favorably with the majority of the existing data on second virial coefficients. The average deviation is approximately equal to the difference in the virial coefficients obtained from the pressure series and the volume series.

- 3) The main sources of error are the pressure and volume measurements. The error in pressure measurement contributes the largest error and is most pronounced at the lower pressures.
- 4) Great care must be taken in operating the apparatus to assure that the piezometer and mercury used in the compression of the vapor sample are free of contamination.
- 5) The Kihara potential was found to fit the second virial coefficients of the pure compounds within experimental error. The results obtained using the Stockmayer potential are not as good but are satisfactory.
- 6) In applying the potential functions to polar-nonpolar binary mixtures the best results were obtained when the homomorph potential parameters were used as nonpolar estimates of the polar potential parameters.
- 7) The unlike molecule interaction in the polar-nonpolar binaries is similar to the interaction of like or unlike nonpolar molecules.

The recommendations for future work on second virial coefficients which were arrived at from this study are:

- 1) An apparatus designed to operate over a much larger temperature range would be very desirable for the following reasons:

a) Before the potential functions can be applied with more meaningful success, experimental data over a range of at least 250 to 300°C will be required.

b) The true temperature behavior of the second virial coefficients and the interaction coefficients could be found from data covering larger temperature ranges.

c) The theoretical treatment of the interaction second virial coefficient could be investigated more thoroughly with data over a wider range of temperatures.

2) Equipment for the improvement of the pressure measurements is now available. Improved pressure measurement would greatly improve the accuracy of the experimental results.

3) The tabulation of the Stockmayer potential values must be expanded before the Stockmayer potential can be applied more completely to the second virial coefficient data of all polar compounds of interest.

A SELECTED BIBLIOGRAPHY

1. Andon, R. J. L, J. D. Cox, E. F. G. Herington and J. F. Martin, Trans. Fara. Soc., 53, 1074(1957)
2. Barker, J. A. and F. Smith, Aus. Journal of Chem., 13, 171(1960)
3. Blanks, B. F. and J. M. Prausnitz, AIChE J., 8, 86(1962)
4. Bottomley, G. A., D. S. Massie and R. Whytlaw-Gray, Proc. Roy. Soc., A, 200, 201(1949)
5. Bottomley, G. A., C. G. Reeves and R. Whytlaw-Gray, Proc. Roy. Soc., A, 246, 505(1958)
6. Casado, F. L., D. S. Massie and R. Whytlaw-Gray, J. Chem. Soc. (London), 1746(1949)
7. Cottrell, T. L. and R. A. Hamilton, Trans. Fara. Soc., 52, 156(1956)
8. Cox, J. D. and R. J. L. Andon, Trans. Fara. Soc., 54, 1622(1958)
9. Documentation Institute, Library of Congress, Doc. 6306
10. Fox, J. H. P. and J. D. Lambert, Proc. Roy. Soc., A, 206, 448(1951)
11. Francis, P. G. and M. L. McGlashan, Trans. Fara. Soc., 51, 593(1955)
12. Gornowski, E. J., E. H. Amick and A. N. Hixson, Ind. Eng. Chem., 39, 1458(1947)
13. Guggenheim, E. A. and M. L. McGlashan, Proc. Roy. Soc., A, 206, 448(1951)
14. Handbook of Chemistry and Physics, Chemical Rubber Publishing Company, 40th Edition(1958)
15. Haselden, G. G., etal., Proc. Roy. Soc., A, 240, 1(1957)

16. Hirschfelder, J. O., C. R. Curtiss and R. B. Bird, "Molecular Theory of Gases and Liquids," (New York) 1954
17. Huff, J. A. and T. M. Reed III, J. Chem. Eng. Data, 8, 306(1963)
18. Jepson, W. B., M. J. Richardson and J. S. Rowlinson, Trans. Fara. Soc., 53, 1586(1957)
19. Jepson, W. B. and J. S. Rowlinson, J. Chem. Phys., 23, 1599(1955)
20. Kihara, T., Rev. Modern Physics, 25, 831(1953)
21. Knoebel, D. H., "An Experimental Investigation of PVT Properties at Low Pressures Using a Modified Boyle's Law Apparatus," M. S. Thesis, Oklahoma State University, Stillwater, Oklahoma(1964)
22. Lambert, J. D., et al, Proc. Roy. Soc., A, 196, 113 (1949)
23. Lambert, J. D. and E. D. T. Strong, Proc. Roy. Soc., A, 200, 566(1950)
24. Lambert, J. D., E. N. Staines and S. D. Woods, Proc. Roy. Soc., A, 200, 262(1950)
25. Lambert, J. D., Disc. Fara. Soc., 15, 226(1953)
26. Lambert, J. D., S. J. Murphy and A. P. Sanday, Proc. Roy. Soc., A, 226 394(1954)
27. Lambert, J. D., et al, Proc. Roy. Soc., A, 249, 414 (1959)
28. Michels, A. and A. J. H. Boerboom, Bull. Soc. Chim. Belges, 62, 119(1953)
29. Pennington, R. E. and K. A. Kobe, J. Am. Chem. Soc., 79, 300(1957)
30. Pitzer, K. S., J. Chem. Phys., 7, 583(1939)
31. Prausnitz, J. M., AIChE J., 5, 3(1959)
32. Rowlinson, J. S., Trans. Fara. Soc., 45, 974(1949)
33. Rowlinson, J. S., Trans. Fara. Soc., 47, 120(1951)

34. Sherwood, A. E. and J. M. Prausnitz, J. Chem. Phys.,
41, 429(1964)
35. Stockmayer, W. H., J. Chem. Phys., 9, 398, 863(1941)
36. Tripp, T. B. and R. D. Dunlap, J. Phys. Chem., 66,
635(1962)
37. Zaalishvili, Sh. D., Zh. Fiz. Khim., 30, 189(1956)

APPENDIX A
PIEZOMETER CALIBRATION

In discussing the calibration of the peizometer, it is first necessary to say a word about the nomenclature which was used. As was mentioned in Chapter III, a volume number is used to designate which calibrated volume is occupied at a given point during a run. Volume number 1 is the total volume of the peizometer, volume number 2 is equal to volume number 1 less the volume of the lower most bulb, volume number 3 is equal to volume 1 less the volume of the lower two bulbs of the piezometer, and so forth to volume number 8 which is the volume of the upper most bulb of the piezometer and the capillary tubing leading to the reference line on the sample side of the mercury manometer. The piezometer bulbs are also numbered consecutively from the bottom, 1 through 8.

The initial calibration was made with distilled, degassed water. After the water was put into the piezometer and allowed to come to room temperature, the contents of each bulb were slowly drained out into separate weighing bottles. The tare and gross weights were obtained on a Mettler gramomatic balance. The density of water at the calibration temperature was found from handbook tabulations (14). Using these densities, the volumes of the individual

bulbs were calculated. These volumes are tabulated in Table A-I.

The volumes to be used in this work were then calculated. Volume number 1 is taken as the total volume. To obtain volume number 2 the volume of bulb number 1 was subtracted from the total volume obtained for each trial. To obtain volume 3 the volume of bulbs 1 and 2 were subtracted from the total volume obtained for each trial. This procedure was used rather than just using the average bulb volumes and the average total volume because it yields a better estimate of the average deviation of the various trials for a given calibration volume. The results of these calculations are presented in Table A-III.

The next step in the calibration was to check the water calibration with runs made with argon at 320 °K where the second virial coefficient of argon is zero (16). These runs yield ratios of the pressure before a compression to the pressure after a compression. Since P_4 or the pressure when volume 4 is occupied, is the highest pressure obtained in several of these runs, this pressure was used as the basis for calculating these ratios. The reason for taking the highest pressure is that this pressure contains the least percentage experimental error. These ratios give seven equations with eight unknowns. Of course, since the second virial coefficient is zero at the temperature of these runs

$$P_4/P_i = V_i/V_4 \quad i \neq 4 \quad (A-1)$$

The ratios of volumes resulting from these runs are presented in Table A-II.

Using the water calibration results for volume number 4 as the basis of calculation, all of the volumes are calculated using the ratios determined from the argon calibrations. The results of these calculations are compared with the results of the water calibration in Table A-III. This comparison shows that the percent deviation from the water calibration is less for most of the volumes than the percent average deviation found between the individual runs of the water calibration. Due to the insignificance of this difference the results arising from the argon calibration were used in conjunction with the one water calibration (volume number 4) in the data reduction portion of this work. The main reason for this is that these volumes were obtained as an average of data which were taken using the technique used in obtaining all the experimental data in this study.

TABLE A-I

WATER CALIBRATION OF PIEZOMETER BULB VOLUMES

Bulb	Volume (cm ³)				Average	Average Dev
	Trial 1	Trial 2	Trial 3	Trial 4		
1	99.7866	99.7650	99.7703	99.7209	99.7584	.0200
2	54.3818	54.3721	54.4266	54.3418	54.3806	.0236
3	31.5406	31.5438	31.5817	31.5229	31.5472	.0172
4	31.8952	31.8562	31.8011	31.8329	31.8464	.0294
5	32.3633	32.3600	32.3546	32.3463	32.3561	.0056
6	7.8058	7.8076	7.8162	7.8143	7.8110	.0042
7	6.4729	6.4748	6.4498	6.4730	6.4676	.0099
8	54.6586	54.6300	54.6455	54.6831	54.6543	.0168
Sum	318.9045	318.8005	318.8450	318.7352	318.8214	.0535

TABLE A-II

VOLUME RATIOS FROM ARGON CALIBRATION

Run Number	V ₁ /V ₄	V ₂ /V ₄	V ₃ /V ₄	V ₅ /V ₄	V ₆ /V ₄	V ₇ /V ₄	V ₈ /V ₄
206	2.39337	1.64447	1.23674				
207	2.39473	1.64432	1.23669				
208	2.39051	1.64566	1.23721	.76080	.51792	.45919	
209	2.39349	1.64500	1.23750	.76071	.51756	.45882	.41038
210	2.39519	1.64507	1.23675	.76081	.51786	.45916	.41055
Avg	2.39436	1.64490	1.23698	.76077	.51778	.45906	.41046

TABLE A-III
COMPARISON OF WATER AND ARGON CALIBRATION

Volume Number	Water Calibration (cm ³)	% Deviation Water Calibration	Argon* Calibration (cm ³)	Percent Difference
1	318.8214	0.0168	318.7736	0.0150
2	219.0630	0.0154	218.9941	0.0314
3	164.6824	0.0163	164.6856	-0.0019
4	133.1352	0.0281	133.1352	-
5	101.2888	0.0194	101.2853	0.0035
6	68.9327	0.0303	68.9347	-0.0029
7	61.1217	0.0358	61.1170	0.0077
8	54.6543	0.0307	54.6467	-0.0139

*Argon calibration is based on volume number 4 of the water calibration.

APPENDIX B
DATA REDUCTION

This appendix deals with the data reduction technique used to obtain the second virial coefficients from the experimental data. A sample of the experimental data is presented in Table B-I.

The technique used was to first calculate the pressures and volumes and then use linear regression to find the second virial coefficient. The pressure is obtained from the following equation:

$$P_n = (R_n - S_n)(E)(F) \quad (B-1)$$

where E, the pressure correction allowing for the cubical expansion of mercury with temperature, is given by:

$$E = 1 / (1 + .18169 \times 10^{-3} T + .2951 \times 10^{-8} T^2 + .1146 \times 10^{-9} T^3) \quad (B-2)$$

and F, the correction for the linear expansion of the cathetometer scale with temperature is given by:

$$F = 1 - 0.000011(t - 20) \quad (B-3)$$

P_n is the pressure for the n^{th} reading (cm Hg)

S_n is the cathetometer reading of the mercury height in the sample leg of the manometer for the n^{th} reading (cm)

TABLE B-I

EXAMPLE OF EXPERIMENTAL DATA

Run 211B Benzene-methanol 47.49 mole % Benzene

Time	Temperature (°C)	Volume Number	R* _n (cm)	S* _n (cm)
11:23	60.00	1	32.130	22.480
11:28	60.00	2	36.500	22.497
11:35	60.00	3	41.082	22.502
11:41	60.00	4	45.467	22.485
11:46	60.00	5	52.610	22.484
11:51	60.00	6	66.475	22.480
11:56	60.00	7	71.985	22.480
12:01	60.00	8	77.735	22.497
12:06	60.00	8	77.732	22.487
12:11	60.00	6	66.480	22.475
12:17	60.00	4	45.452	22.480
12:24	60.00	2	36.485	22.475
12:30	60.00	1	32.145	22.490

*These values are the average of two or three cathetometer readings.

R_n is the cathetometer reading of the mercury height in the vacuum leg of the manometer for the n^{th} reading (cm).

T is the bath temperature ($^{\circ}\text{C}$).

t is the room temperature ($^{\circ}\text{C}$).

k is the total number of readings or datum points recorded during a run.

No correction was made for the effect of the vapor pressure of mercury. It has been shown (18,19) that under conditions such as those in this study the actual effect of the mercury is much less than the vapor pressure and therefore should be neglected.

The volumes are corrected for deviation of the mercury height from the reference mark on the sample side of the manometer. In making this correction to the volume it is assumed that the average of the mercury height readings on the sample side of the manometer, S_n , is equal to the cathetometer reading of the reference mark. The corrected volumes are then given by:

$$V_n = V_{n,\text{calibrated}} + (S_{n,\text{avg}} - S_n)0.7854 \quad (\text{B-4})$$

where

V_n is the volume occupied at the n^{th} reading (cm^3).

$V_{n,\text{calibrated}}$ is the calibrated volume occupied at the n^{th} reading (cm^3).

$S_{n,\text{avg}}$ is the arithmetic average of S_n (cm).

and the factor 0.7854 is the cross sectional area of the sample leg of the manometer (cm^2).

After the pressures and the volumes are calculated using the above equations, a least square analysis is used

to find the best fit of the following linear equation:

$$P_n V_n = NR_o(T + 273.16) + NB'P_n \quad (B-5)$$

where N is the number of moles (g-moles), R_o is the universal gas constant (cm Hg-cm³/g-mole °K), and B' is the second virial coefficient (ml/g-mole). The following equations are used to find the best fit:

$$NB' = \frac{\sum_{n=1}^k (P_n V_n) P_n - \left(\sum_{n=1}^k P_n V_n \sum_{n=1}^k P_n \right) / k}{\sum_{n=1}^k (P_n)^2 - \left(\sum_{n=1}^k P_n \right)^2 / k} \quad (B-6)$$

$$NR_o(T + 273.16) = \left(\sum_{n=1}^k P_n V_n - NB' \sum_{n=1}^k P_n \right) / k \quad (B-7)$$

The two unknowns in the above equations (N and B') can be determined.

An IBM 1410 digital computer program was used to make these calculations. An error analysis based on the deviations of the experimental $P_n V_n$ from the fitted straight line was included in this program. The results of this analysis are presented in Appendix D. For comparison purposes the above program also calculated the second virial coefficients obtained from the following form of the virial equation of state:

$$P_n V_n = NR_o(T + 273.16)(1 + NB/V_n) \quad (B-8)$$

This equation was fitted by least square linear regression using equations similar to Equations B-6 and B-7 except that P_n is replaced by $1/V_n$ in all terms other than the those containing the $P_n V_n$ product.

The calculated results for all runs made in this study are presented in Tables B-II through B-X. The temperatures given are the average measured temperatures during a run. The maximum deviation from the average was 0.05 °C. The compositions presented were determined by weighing the constituents together using a Mettler Grammatic balance.

TABLE B-II
RESULTS FOR BENZENE

Run Number	Temperature (°C)	Second Virial Coefficient (ml/mole)	
		P-series	1/V-series
204	39.99	-1279	-1262
391	40.02	-2061	-2016
392	40.01	-3106	-3004
202	60.05	-1166	-1136
203	60.05	-1116	-1089
205	59.97	-1105	-1086
253	59.97	-1068	-1043
254	59.97	-1127	-1103
262	59.98	-1465	-1424
263	60.03	-1522	-1477
264	60.05	-1481	-1438
265	59.97	-1121	-1094
266	59.97	-1004	-986
Test	60.00	-1133	-1108
280	79.92	-892	-874
281	79.98	-852	-838
311	80.03	-920	-904
312	80.02	-1065	-1047
371	80.01	-921	-901
372	80.02	-907	-891
329	100.05	-769	-756
330	100.07	-774	-764

TABLE B-III
RESULTS FOR METHANOL

Run Number	Temperature (°C)	Second Virial Coefficient (ml/mole)	
		P-series	1/V-series
218	39.98	-2323	-2245
219	39.98	-2187	-2129
226	39.99	-2613	-2570
227A	39.98	-1971	-1928
389	39.98	-2711	-2601
390	39.99	-3184	-3075
220	59.99	-1086	-1069
221	60.04	-1259	-1222
227B	59.97	-1067	-1047
228	59.97	-1054	-1033
292	60.02	-1266	-1227
293	59.98	-1140	-1114
308	59.98	-1084	-1061
309A	59.97	-1149	-1126
387	59.97	-1580	-1500
388	59.98	-1498	-1428
286	79.96	-755	-738
287	79.95	-721	-709
290	79.93	-762	-743
291	79.92	-769	-754
309B	80.03	-763	-746
310	80.03	-742	-729
335	100.07	-505	-498
336	100.07	-544	-536

TABLE B-IV
RESULTS FOR ETHANOL

Run Number	Temperature (°C)	Second Virial Coefficient (ml/mole)	
		P-series	1/V-series
233	59.97	-1485	-1450
234	59.97	-1560	-1521
284	79.94	-1030	-1003
285	79.92	-972	-952
313	80.02	-982	-957
314	80.03	-1003	-980
373	80.02	-930	-913
374	80.02	-931	-914
381	80.02	-915	-895
382	80.05	-862	-847
331	100.55	-683	-674
332	100.07	-691	-683

TABLE B-V
RESULTS FOR ACETONE

Run Number	Temperature (°C)	Second Virial Coefficient (ml/mole)	
		P-series	1/V-Series
239B	40.00	-1701	-1638
240A	39.99	-1678	-1622
394	39.98	-3694	-3589
239A	59.97	-1259	-1225
240B	59.97	-1267	-1235
282	79.99	-1051	-1021
283	79.92	-995	-972
288	80.02	-1007	-984
289	80.02	-932	-916
315	80.02	-1027	-999
316	80.02	-994	-973
369	79.94	-1034	-1010
370	80.01	-1004	-985
337	100.09	-838	-818
338	100.07	-826	-810
349	100.06	-842	-824
350	100.07	-831	-817

TABLE B-VI
RESULTS FOR DIETHYL ETHER

Run Number	Temperature (°C)	Second Virial Coefficient (ml/mole)	
		P-series	1/V-series
259	59.99	-952	-939
260	59.98	-861	-846
261	59.97	-955	-940
267	59.97	-873	-857
276	59.97	-832	-818
277	59.97	-787	-777
278	79.95	-729	-717
279	79.97	-641	-634
375	80.03	-650	-641
376	80.02	-689	-681
333	100.07	-554	-547
334	100.08	-495	-491

TABLE B-VII
RESULTS FOR BENZENE-METHANOL

Run Number	Temperature (°C)	Mole Fraction Benzene	Second Virial Coefficient (ml/mole)	
			P-series	1/V-series
211A	39.98	.4749	-1091	-1069
212B	39.98	.4749	-1106	-1086
213A	40.00	.3147	-1321	-1292
214B	39.99	.3147	-1307	-1283
215A	40.00	.6379	-1091	-1075
216B	40.00	.2039	-1536	-1503
217A	40.02	.2039	-1508	-1475
222B	40.06	.7717	-1427	-1404
223A	40.05	.7717	-1134	-1116
211B	59.97	.4749	-802	-781
212A	59.98	.4749	-784	-769
213B	59.99	.3147	-857	-838
214A	59.97	.3147	-815	-800
215B	60.07	.6379	-838	-826
216A	60.04	.2039	-1008	-980
217B	60.07	.2039	-933	-913
222A	60.04	.7717	-848	-838
223B	59.97	.7717	-916	-903
224A	60.00	.7239	-813	-801
225B	59.97	.7239	-895	-881
255	59.99	.4617	-791	-774
256	59.97	.4617	-759	-747
257	59.98	.4617	-775	-764
224B	80.04	.7239	-727	-716
225A	79.99	.7239	-735	-726
323	80.02	.1843	-635	-623
324	80.03	.1843	-622	-611
325	80.00	.4349	-588	-578
326	80.03	.4349	-574	-566
327	80.03	.6521	-639	-628
328	80.01	.6521	-568	-561
377	80.03	.5334	-594	-585
378	80.04	.5334	-582	-574
379	80.02	.2380	-635	-623
380	80.03	.2380	-568	-559
385	80.03	.6979	-642	-631
386	80.03	.6979	-656	-646
355	100.07	.1903	-424	-419
356	100.07	.1903	-443	-437
357	100.07	.4638	-471	-464
358	100.07	.4638	-486	-479
359	100.07	.6961	-571	-562
360	100.07	.6961	-580	-573

TABLE B-VIII
RESULTS FOR BENZENE-ETHANOL

Run Number	Temperature (°C)	Mole Fraction Benzene	Second Virial Coefficient (ml/mole)	
			P-series	1/V-series
229	59.97	.7305	-909	-894
230B	59.97	.7305	-917	-903
231	59.97	.5712	-926	-909
232	59.97	.5712	-917	-903
235	59.97	.4071	-953	-936
236	59.98	.4071	-1005	-987
237	59.97	.2684	-1135	-1110
238	59.97	.2684	-1143	-1117
230A	80.00	.7305	-859	-849
296	79.94	.2033	-760	-750
297	79.93	.2033	-758	-747
298	80.03	.5168	-672	-662
299	80.04	.5168	-693	-685
300	80.04	.7112	-735	-723
301	80.02	.7112	-747	-739
363	100.07	.2071	-660	-650
364	100.07	.2071	-633	-624
365	100.07	.5475	-627	-616
366	100.07	.5475	-632	-623
367	100.08	.7067	-682	-670
368	100.07	.7067	-615	-607

TABLE B-IX
RESULTS FOR BENZENE-ACETONE

Run Number	Temperature (°C)	Mole Fraction Benzene	Second Virial Coefficient (ml/mole)	
			P-series	1/V-series
242B	40.00	.7765	-1398	-1373
243	39.98	.7765	-1592	-1564
244	39.98	.5198	-1446	-1420
245A	40.00	.5198	-1609	-1585
248B	40.00	.4128	-1473	-1438
249	39.98	.4128	-1470	-1442
250	39.98	.2277	-1498	-1460
251A	39.98	.2277	-1487	-1449
241	59.97	.7765	-1022	-1006
242A	59.97	.7765	-1042	-1027
245B	59.99	.5198	-1243	-1229
246	59.97	.5198	-1092	-1075
247	59.97	.4128	-1073	-1050
248A	59.98	.4128	-1081	-1062
251B	59.97	.2277	-1145	-1123
252	59.97	.2277	-1095	-1077
317	80.03	.2531	-919	-896
318	80.02	.2531	-905	-887
319	80.03	.5301	-841	-824
320	80.03	.5301	-881	-866
321	80.03	.6991	-822	-807
322	80.02	.6991	-824	-811
383	80.03	.6947	-798	-783
384	80.04	.6947	-832	-819
347	100.07	.2438	-766	-750
348	100.07	.2438	-739	-727
351	100.05	.5019	-719	-706
352	100.07	.5019	-709	-698
353	100.08	.7405	-749	-735
354	100.07	.7405	-719	-707
361	100.08	.7122	-716	-703
362	100.06	.7122	-702	-693

TABLE B-X
RESULTS FOR BENZENE-DIETHYL ETHER

Run Number	Temperature (°C)	Mole Fraction Benzene	Second Virial Coefficient (ml/mole)	
			P-series	1/V-series
268	59.97	.6800	-993	-973
269	59.97	.6800	-933	-918
270	59.97	.5057	-880	-864
271	59.97	.5057	-890	-877
272	59.97	.4124	-972	-952
273	59.97	.4124	-885	-870
274	59.97	.2890	-842	-828
275	59.98	.2890	-889	-876
294	59.97	.7915	-971	-954
295	59.97	.7915	-986	-971
302	80.03	.5365	-783	-771
303	80.02	.5365	-847	-836
304	80.02	.2726	-738	-728
305	80.02	.2726	-730	-722
306	80.06	.7978	-864	-849
307	80.02	.7978	-856	-843
339	100.07	.2516	-645	-636
340	100.08	.2516	-655	-647
341	100.07	.5342	-651	-641
342	100.07	.5342	-650	-642
343	100.05	.8052	-711	-700
344	100.07	.8052	-701	-692
345	100.10	.2461	-619	-611
346	100.07	.2461	-661	-654

APPENDIX C
CALCULATION PROCEDURE USED TO DETERMINE
THE INTERACTION SECOND VIRIAL
COEFFICIENTS- B_{12}

The calculation of B_{12} was accomplished using a least squares determination of the one unknown constant, B_{12} , in the following equation:

$$B_M = x^2 B_{11} + 2x(1-x)B_{12} + (1-x)^2 B_{22} \quad (C-1)$$

where B_M , x , B_{11} and B_{22} are experimentally known quantities.

Since the least squares involves the determination of only one constant, it is a unique calculation. An IBM 1410 digital computer program was used for the above calculation. The predicted values of B_M using the determined value of B_{12} were also calculated with this program at $x = .1, .2, .3, .4, .5, .6, .7, .8, \text{ and } .9$ to facilitate drawing of the calculated virial coefficient curves appearing in Figures VII through X in Chapter V.

The results of the above calculations are presented in Tables C-I through C-IV. The B(obs) values are experimental, B(calc) values are calculated using Equation C-1, and the Dev values are the deviations between the experimental and calculated values.

TABLE C-I
RESULTS OF B_{12} CALCULATIONS FOR THE
BENZENE-METHANOL SYSTEM

Mole Fraction Benzene	Temperature (°C)	B(obs) (ml/mole)	B(calc) (ml/mole)	Dev (ml/mole)
1.0000	40.0	-1303		
.0000		-2079		
.4749		-1099	-1139	-40
.3147		-1314	-1341	-27
.6379		-1091	-1055	36
.2039		-1522	-1549	-27
.7717		-1134	-1077	57
$B_{12} = -545$ ml/mole				
1.0000	60.00	-1107		
.0000		-1097		
.4749		-793	-805	-12
.3147		-837	-843	-6
.6379		-838	-828	9
.2039		-970	-906	64
.7717		-882	-895	-13
.7239		-854	-866	-12
.4617		-775	-806	-31
$B_{12} = -507$ ml/mole				
1.0000	80.00	-944		
.0000		-752		
.7239		-731	-680	51
.1843		-628	-628	-
.4349		-581	-576	5
.6521		-603	-637	-34
.5334		-588	-591	-3
.2380		-601	-606	-5
.6979		-649	-663	-14
$B_{12} = -319$ ml/mole				
1.0000	100.00	-815		
.0000		-524		
.1903		-434	-460	-26
.4638		-478	-466	12
.6961		-576	-562	14
$B_{12} = -281$ ml/mole				

TABLE C-II
 RESULTS OF B_{12} CALCULATIONS FOR THE
 BENZENE-ETHANOL SYSTEM

Mole Fraction Benzene	Temperature (°C)	B(obs) (ml/mole)	B(calc) (ml/mole)	Dev (ml/mole)
1.0000	60.00	-1107		
.0000		-1522		
.7305		-913	-925	-12
.5712		-922	-919	3
.4071		-979	-992	-13
.2684		-1139	-1117	22
	$B_{12} = -567$ ml/mole			
1.0000	80.00	-944		
.0000		-941		
.2033		-759	-773	-14
.5168		-683	-682	1
.7112		-742	-729	13
	$B_{12} = -421$ ml/mole			
1.0000	100.00	-815		
.0000		-687		
.2071		-647	-628	19
.5475		-629	-628	1
.7067		-649	-669	-20
	$B_{12} = -490$ ml/mole			

TABLE C-III
 RESULTS OF B_{12} CALCULATIONS FOR THE
 BENZENE-ACETONE SYSTEM

Mole Fraction Benzene	Temperature (°C)	B(obs) (ml/mole)	B(calc) (ml/mole)	Dev (ml/mole)
1.0000	40.00	-1303		
.0000		-1690		
.7765		-1397	-1348	49
.5198		-1446	-1428	18
.4128		-1471	-1472	-1
.2277		-1493	-1559	-66
	$B_{12} = -1376$ ml/mole			
1.0000	60.00	-1107		
.0000		-1263		
.7765		-1032	-1053	-21
.5198		-1092	-1055	37
.4128		-1077	-1075	2
.2277		-1120	-1138	-18
	$B_{12} = -930$ ml/mole			
1.0000	80.00	-944		
.0000		-1005		
.2530		-912	-885	27
.5301		-861	-835	26
.6991		-823	-846	-23
.6947		-815	-845	-30
	$B_{12} = -698$ ml/mole			
1.0000	100.00	-815		
.0000		-834		
.2438		-752	-744	8
.5019		-714	-709	5
.7405		-734	-731	3
.7122		-709	-726	-17
	$B_{12} = -593$ ml/mole			

TABLE C-IV
 RESULTS OF B_{12} CALCULATIONS FOR THE
 BENZENE-DIETHYL ETHER SYSTEM

Mole Fraction Benzene	Temperature (°C)	B(obs) (ml/mole)	B(calc) (ml/mole)	Dev (ml/mole)
1.0000	60.00	-1107		
.0000		-895		
.6800		-963	-945	18
.5057		-885	-894	-9
.4124		-885	-878	7
.2890		-865	-868	-2
.7915		-979	-992	-13
		$B_{12} = -785$ ml/mole		
1.0000	80.00	-944		
.0000		-677		
.5365		-815	-799	16
.2726		-734	-733	1
.7978		-860	-876	-16
		$B_{12} = -769$ ml/mole		
1.0000	100.00	-815		
.0000		-525		
.5342		-651	-655	-4
.8052		-706	-743	-37
.2461		-619	-578	41
		$B_{12} = -620$ ml/mole		

APPENDIX D

ERROR ANALYSIS

In the reduction of the data to determine second virial coefficients a least square regression analysis is used. Therefore a standard estimate of error for the determined second virial coefficients can be found from statistical methods. This analysis does not indicate the existence of adsorption of the sample due to contamination. Visual inspection of a plot of PV versus P is necessary for this. This analysis does account for possible error in B due to the deviations or scatter of the PV versus P data. The following analysis assumes negligible error in P. On the basis of the magnitude of the respective errors in P and PV this assumption is valid. The following equations are used to calculate the various errors from the least squares analysis of the experimental data:

The standard error in the PV values is given by

$$S_{pv} = \left\{ \frac{k \sum (P_n V_n)^2 - (\sum P_n V_n)^2}{k(k-2)} \right\}^{1/2} \quad (D-1)$$

The standard error in the intercept, S_A , is then given by

$$S_A = S_{pv} \left\{ \frac{\sum P_n}{k \sum P_n - (\sum P_n)} \right\}^{1/2} \quad (D-2)$$

and the standard error in the slope, S_B , by

$$S_B = S_{pv} \left\{ \frac{k}{k \sum P_n - (\sum P_n)} \right\}^{1/2} \quad (D-3)$$

Using the above equations and an assumed standard error in the temperature, S_T , of 0.03°C the standard error in B can be calculated as follows:

Since

$$B = \text{Slope/Intercept/RT} \quad (D-4)$$

if the standard errors are converted to percent errors, the percent standard error in B is

$$\text{Pct. Std. Error in B} = (S_A/NRT + S_B/NB + S_T/T)100 \quad (D-5)$$

The standard error in B can now be obtained by multiplying the percent error times the value of B. These calculations were made as part of the digital computer program used in the data reduction. The results are listed in Tables D-I through D-IX.

To check the validity of this method of analysis most of the experimental data were obtained in duplicate. From these duplicates an average deviation in B can be

TABLE D-I
 ERROR ANALYSIS RESULTS FOR BENZENE DATA

Run Number	Sample Size (g-mole x 10 ⁴)	Intercept (cm Hg-ml)	Standard Error in PV (cm Hg-ml)	Standard Error in B (ml/mole)
204	7.46	1457	0.45	58
391	5.19	1014	1.29	160 (a)
392	6.62	1293	3.11	402 (a)
202	9.67	2009	0.54	25
203	9.76	2029	1.01	25
205	7.00	1455	0.38	28
253	11.10	2306	0.94	25
254	9.14	1899	1.39	52 (b)
262	9.03	1875	1.67	68 (b)
263	9.13	1896	1.40	59 (b)
264	10.37	2154	1.96	72 (b)
265	10.46	2174	0.72	20
266	8.57	1779	0.60	28
Test	8.84	1837	0.55	27
280	10.92	2406	0.69	17
281	8.84	1956	0.71	27
311	9.03	1989	1.28	48
312	7.37	1623	0.85	56
371	11.65	2567	1.45	32
372	9.25	2038	1.33	46
329	10.12	2355	0.96	31
330	8.29	1929	1.75	70 (a)

(a) Deleted- error in PV exceeded maximum expected error.

(b) Deleted- system known to be contaminated.

TABLE D-II
 ERROR ANALYSIS RESULTS FOR METHANOL DATA

Run Number	Sample Size (g-mole x 10 ⁴)	Intercept (cm Hg-ml)	Standard Error in PV (cm Hg-ml)	Standard Error in B (ml/mole)
218	16.44	3211	1.61	112
219	12.31	2404	1.27	115
226	2.89	564	0.74	336 (a)
227A	8.80	1719	0.42	42
389	11.74	2293	1.65	101 (a)
390	7.17	1399	12.26	1041 (a)
220	6.85	1423	0.86	59
221	12.70	2638	1.44	33
227B	8.79	1827	0.71	27
228	9.06	1882	0.74	29
292	11.78	2448	1.25	29
293	9.66	2006	0.64	22
308	15.06	3129	0.92	37
309	13.98	2904	0.96	44
387	16.01	3326	5.18	66 (a)
388	16.78	3487	5.40	71 (a)
286	13.99	3082	0.99	15
287	11.33	2495	1.52	35 (a)
290	15.02	3308	1.17	16
291	12.08	2660	1.17	24
309B	13.98	3079	1.44	22
310	11.29	2487	0.93	22
335	13.92	3240	1.88	27 (a)
336	12.49	2908	0.79	14

TABLE D-III
ERROR ANALYSIS RESULTS FOR ETHANOL DATA

Run Number	Sample Size (g-mole $\times 10^4$)	Intercept (cm Hg-ml)	Standard Error in PV (cm Hg-ml)	Standard Error in B (ml/mole)
233	9.93	2064	1.07	52
234	9.99	2076	0.73	36
284	12.11	2666	0.97	20
285	10.15	2235	1.10	32
313	12.29	2706	1.11	22
314	11.16	2458	1.19	29
373	9.47	2087	0.95	31
374	9.02	1988	0.89	32
381	10.65	2347	0.75	21
382	9.86	2171	0.99	30
331	8.12	1890	0.79	39
332	8.16	1900	0.70	29

TABLE D-IV
 ERROR ANALYSIS RESULTS FOR ACETONE DATA

Run Number	Sample Size (g-mole x 10 ⁴)	Intercept (cm Hg-ml)	Standard Error in PV (cm Hg-ml)	Standard Error in B (ml/mole)
239B	10.67	2083	0.51	17
240A	9.32	1820	0.27	12
394	6.18	1207	1.39	349 (a)
239A	10.67	2217	0.78	21
240B	9.33	1938	0.42	16
282	13.17	2900	0.91	16
283	10.79	2377	1.19	30
288	10.31	2270	0.81	25
289	8.45	1860	1.15	52
315	12.98	2858	1.00	18
316	10.28	2264	0.89	25
369	10.48	2309	0.53	15
370	9.11	2007	1.20	42
337	13.71	3192	1.38	21
338	10.88	2531	1.51	36 (a)
349	11.84	2756	1.31	29
350	9.70	2257	1.28	41

TABLE D-V
ERROR ANALYSIS RESULTS FOR DIETHYL ETHER DATA

Run Number	Sample Size (g-mole $\times 10^4$)	Intercept (cm Hg-ml)	Standard Error in PV (cm Hg-ml)	Standard Error in B (ml/mole)
258	7.19	1494	0.66	40
259	7.05	1464	1.16	73
260	9.23	1918	1.17	43
261	7.98	1657	1.16	57
267	9.28	1929	0.42	17
276	9.58	1991	0.61	21
277	7.96	1654	0.42	21
278	10.60	2334	0.92	24
279	8.71	1918	0.56	22
375	9.32	2052	0.75	25
376	7.65	1685	1.24	61
333	9.88	2299	0.99	32
334	8.12	1890	0.92	40

TABLE D-VI

ERROR ANALYSIS RESULTS FOR BENZENE-METHANOL DATA

Run Number	Sample Size (g-mole x 10 ⁴)	Intercept (cm Hg-ml)	Standard Error in PV (cm Hg-ml)	Standard Error in B (ml/mole)
211A	14.71	2871	0.63	22
212B	11.96	2335	0.40	34
213A	12.74	2487	0.82	39
214B	10.94	2136	0.73	47
215A	8.08	1577	0.53	45
216B	13.90	2417	0.71	50
217A	11.43	2232	0.91	53
222B	6.74	1315	0.72	84
223A	7.70	1504	0.47	46
211B	14.69	3052	1.40	20
212A	11.96	2482	1.29	28
213B	12.72	2643	0.83	15
214A	10.92	2269	0.64	16
215B	8.08	1678	1.47	70 (a)
216A	13.88	2885	1.44	23
217B	11.42	2372	0.82	19
222A	6.72	1397	0.42	32
223B	7.70	1600	0.94	49
224A	8.76	1819	0.61	25
225B	8.14	1692	0.53	24
255	12.65	2628	0.70	14
256	10.40	2160	0.70	20
257	8.58	1782	0.62	26
224B	8.76	1929	0.39	18
225A	8.14	1793	0.54	25
323	13.83	3047	1.55	24
324	12.89	2840	0.97	17
325	14.75	3249	1.07	15
326	11.67	2571	0.94	20
327	12.56	2766	1.08	21
328	10.32	2272	1.05	29
377	12.23	2694	0.99	19
378	10.03	2209	0.59	17
379	15.64	3446	1.19	16
380	12.37	2724	1.08	22
385	12.31	2712	1.13	22
386	10.08	2220	1.39	44
355	14.47	3368	1.69	25
356	15.42	3589	1.78	23
357	13.93	3243	1.53	24
358	11.72	2727	0.98	23
359	12.97	3018	1.76	34
360	10.22	2380	0.96	35

TABLE D-VII

ERROR ANALYSIS RESULTS FOR BENZENE-ETHANOL DATA

Run Number	Sample Size (g-mole x 10 ⁴)	Intercept (cm Hg-ml)	Standard Error in PV (cm Hg-ml)	Standard Error in B (ml/mole)
229	9.03	1875	0.33	13
230B	7.32	1521	0.43	28
231	10.22	2125	0.54	16
232	8.34	1734	0.51	22
235	10.83	2250	0.37	16
236	8.85	1838	0.88	34
237	11.56	2402	0.75	27
238	9.86	2049	0.95	29
230A	7.34	1616	0.90	64
296	8.66	1907	0.83	34
297	9.51	2095	0.81	28
298	9.60	2115	0.69	26
299	7.86	1732	0.52	27
300	9.30	2049	0.72	29
301	7.63	1680	0.54	32
363	10.85	2526	0.88	23
364	9.57	2227	0.73	24
365	12.46	2901	1.27	27
366	10.14	2359	0.89	26
367	12.11	2819	0.96	22
368	9.92	2308	0.81	24

TABLE D-VIII

ERROR ANALYSIS RESULTS FOR BENZENE-ACETONE DATA

Run Number	Sample Size (g-mole x 10 ⁴)	Intercept (cm Hg-ml)	Standard Error in PV (cm Hg-ml)	Standard Error in B (ml/mole)
242B	6.43	1255	0.75	71
243	5.29	1032	1.08	132 (a)
244	9.93	1939	1.15	88
245A	4.51	881	0.69	116
248B	7.96	1554	1.08	55
249	6.54	1277	0.92	70
250	8.04	1569	0.82	45
251A	8.44	1647	1.09	50
241	7.85	1631	0.61	30
242A	6.43	1336	0.55	46
245B	4.52	938	0.52	81
246	6.72	1396	0.56	43
247	9.73	2022	0.83	27
248A	7.97	1655	0.94	45
251B	8.45	1756	0.68	29
252	6.92	1438	0.38	26
317	13.50	2975	0.83	14
318	10.74	2365	1.16	30
319	11.28	2485	0.83	19
320	9.24	2035	1.53	53 (a)
321	10.81	2382	0.70	18
322	8.90	1961	0.84	31
383	11.06	2437	0.95	24
384	9.09	2002	1.18	42
347	12.26	2853	1.11	22
348	10.11	2352	1.02	33
351	12.16	2831	1.17	22
352	10.02	2332	1.05	32
353	11.99	2792	0.90	18
354	9.84	2291	0.93	31
361	11.44	2663	1.18	30
362	9.06	2109	1.22	41

TABLE D-IX

ERROR ANALYSIS RESULTS FOR BENZENE-DIETHYL ETHER DATA

Run Number	Sample Size (g-mole x 10 ⁴)	Intercept (cm Hg-ml)	Standard Error in PV (cm Hg-ml)	Standard Error in B (ml/mole)
268	9.70	2016	0.60	20
269	7.99	1660	0.41	22
270	9.56	1987	0.55	21
271	7.79	1619	0.47	24
272	10.29	2137	0.73	22
273	8.51	1768	0.39	19
274	9.47	1967	0.63	22
275	7.75	1611	0.92	47
294	8.92	1853	0.82	33
295	7.32	1522	0.44	28
302	8.82	1943	0.80	33
303	7.23	1593	0.91	50
304	7.96	1753	0.62	31
305	6.54	1440	0.85	68
306	8.91	1963	0.28	13
307	7.32	1613	0.73	47
339	10.23	2382	1.12	32
340	8.39	1954	0.97	38
341	11.13	2591	1.89	42 (a)
342	9.12	2122	1.03	37
343	11.00	2559	1.69	39 (a)
344	9.07	2112	0.97	32
345	9.97	2320	1.18	33
346	8.19	1906	1.23	50

obtained as follows:

$$\text{Avg dev in B} = \frac{\sum (B_1 - B_2)/2}{m} \quad (\text{D-6})$$

where B_1 and B_2 are the duplicate values of B and m is the total number of duplicates considered. The above was used for the binary mixtures. For the pure components the average value of B was calculated from the runs made at a given temperature and the deviations from these average values were calculated.

For the pure components the average deviation of B found from 71 runs was ± 29.4 ml/mole. For the duplicate runs made on the mixtures, the average deviation of 54 sets of duplicates was found to be ± 13.4 ml/mole. The average standard error in B found from the statistical treatment was 32.1 ml/mole. This comparison shows that it is acceptable to use the statistical treatment to determine the validity of individual runs.

The average deviation and the standard deviation in PV are also obtained from the error analysis. It is of interest to see if the standard deviation of PV observed from experiment can be accounted for by known errors in the experimental measurements. This latter error will be referred to as the expected error.

The expected error in the PV product can be calculated from the errors associated with the various measurements

used to obtain the data. The maximum error in the volume is assumed to be the maximum average deviation from the volume calibration. From Table A-III this is found to be 0.036%. The error in the pressure measurement is due to the inaccuracy associated with reading the cathetometer. This accuracy is .003 cm and since two cathetometer readings are required for the pressure, the expected error in the pressure is .006 cm. This amounts to .06% at 10 cm Hg pressure and .015% at 40 cm Hg pressure. The sum of the percent errors associated with the volume and pressure yields the percent expected error in PV. This percentage error as a function of pressure is shown in Figure D-1. This actually is pessimistic since the error in the volume is less than .036 ml for the case of largest volume, i.e. lowest pressure.

Figure D-2 shows the expected percent average deviation of PV for a run of eight pressure measurements versus the approximate magnitude of PV. It is seen from this figure that as the sample size is decreased, magnitude of PV becomes less, the expected average percent deviation becomes greater. This is due to the decrease in the magnitude of the pressure for small samples. The average standard deviation found from the analysis of the experimental data was 0.88 cm Hg-ml. This would amount to an average percent deviation of .08%, .044% and .030% for PV equal to 1000, 2000 and 3000 respectively. These are all

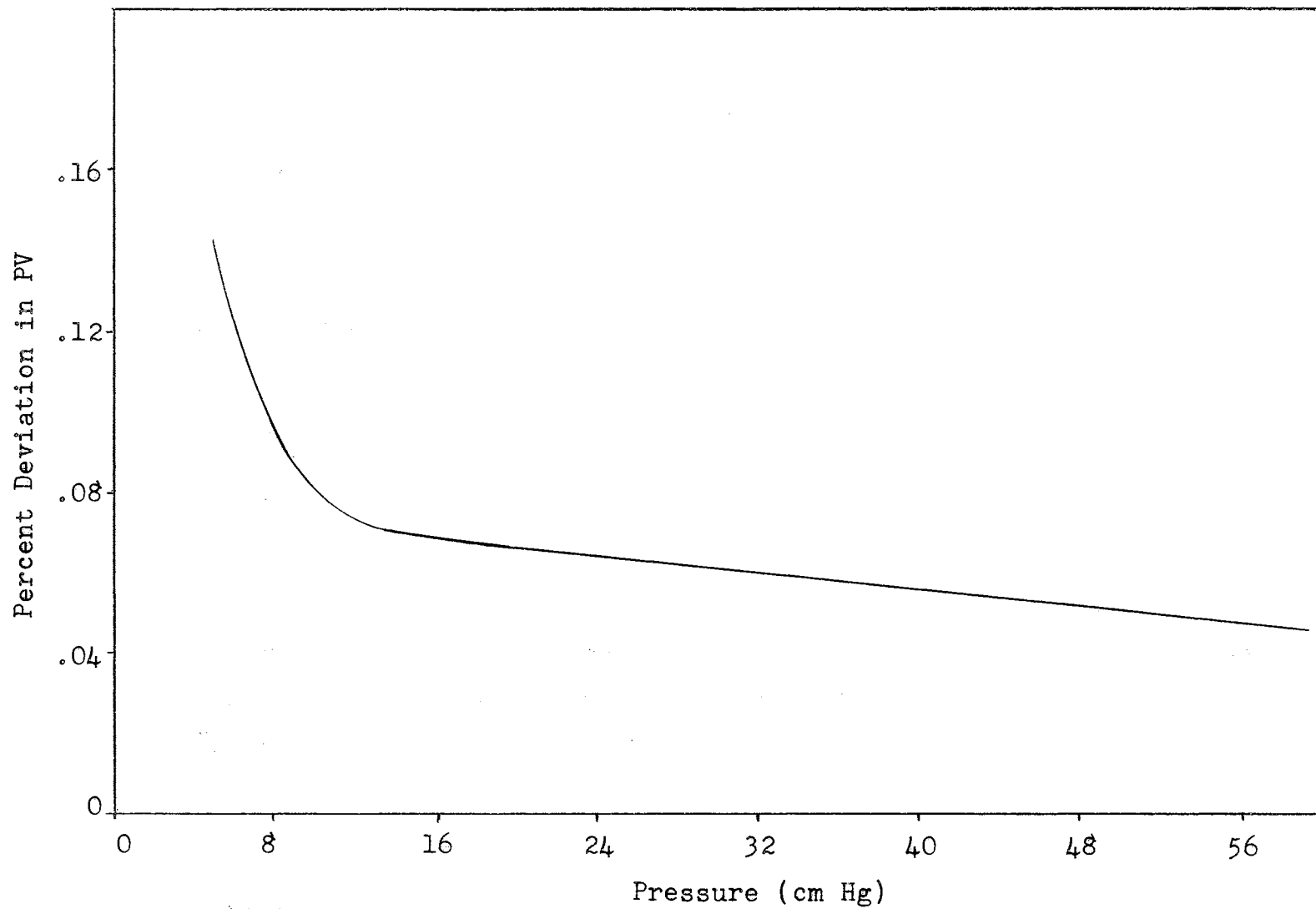


Figure D-1. Expected Percent Deviation in PV as a Function of Pressure

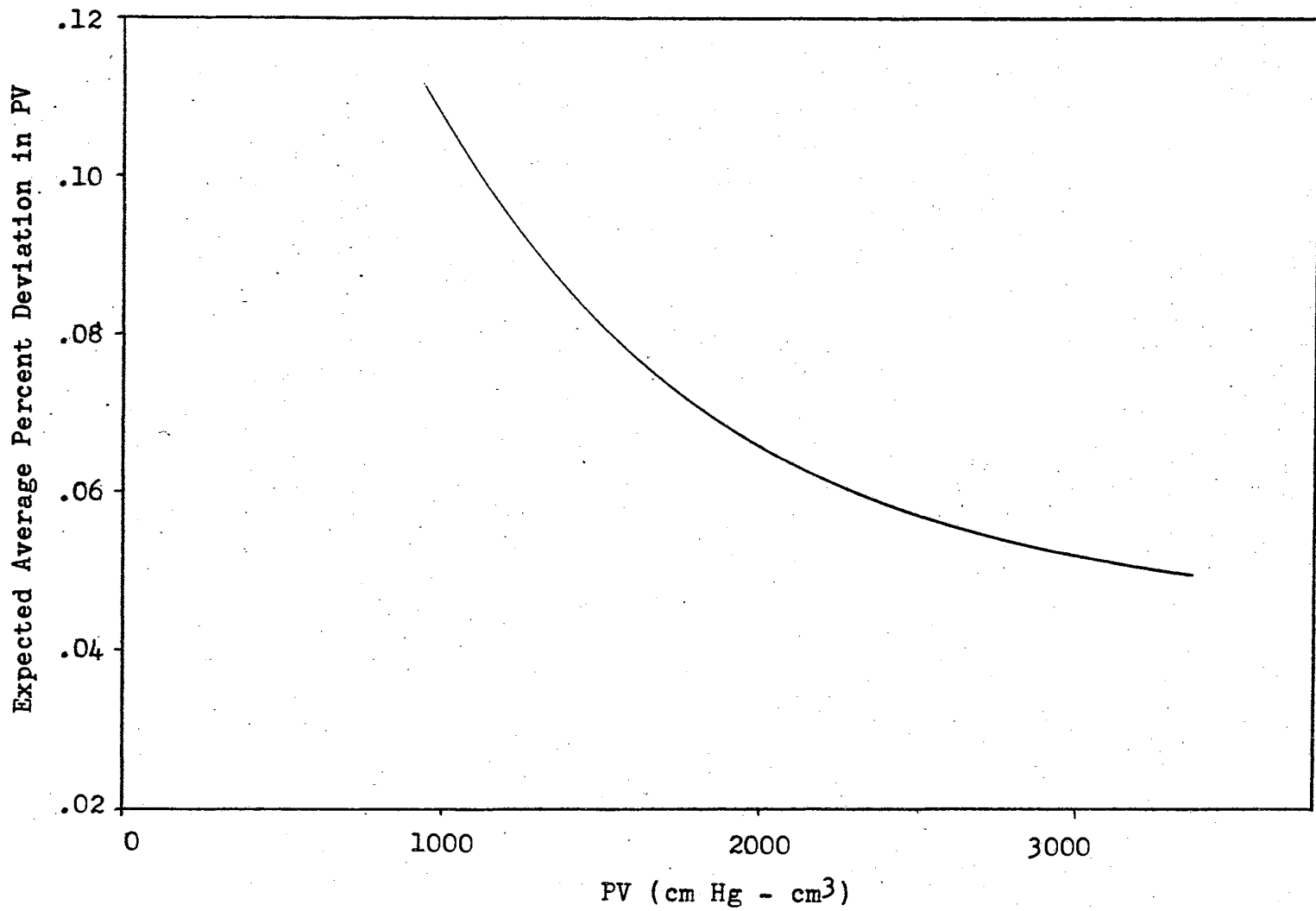


Figure D-2. Average Expected Percent Deviation in PV of Eight Measurements versus the Magnitude of PV

less than the values given in Figure D-2 which of course is expected. On the basis of this analysis several experimental runs were discounted as indicated in Tables D-I through D-IX.

APPENDIX E

CALCULATION OF INTERMOLECULAR PARAMETERS FROM EXPERIMENTAL DATA

There are several ways in which the intermolecular parameters can be calculated from experimental data. These vary from a graphical procedure used primarily before the advent of digital computers to the use of least squares analysis. The method used in this work is the latter. The main reason for using this method is that a great quantity of experimental data can be examined in a relatively short period of time.

The integrated forms of the potential functions and the information available for each of them will be discussed before discussing the least square analysis.

Lennard-Jones Potential

Integration of Equation (7) with the potential energy given by Equation 8, gives the following form of the Lennard-Jones potential:

$$B(T) = b_0 B^*(T^*) \quad (E-1)$$

where $b_0 = 2/3 N^3$ and $T^* = kT/\epsilon$. Values of B^* are tabulated in the literature (16) for values of T^* ranging

from 0.1 to 1000.

Stockmayer Potential

Upon substitution of Equation (9) into Equation (6) and integrating the following representation of the Stockmayer potential is obtained:

$$B(T) = b_0 B^*(T^*, t^*) \quad (E-2)$$

where $t^* = \mu^2 / \sqrt{8\epsilon\sigma^3}$ and the remaining terms are the same as above. There are tabulations of $B^*(T^*, t^*)$ in the literature (16) for values of T^* ranging from 0.30 to 400 and values of t^* ranging from 0.1 to 2.4.

Kihara Potential

In order to obtain an expression similar to those above for the Kihara potential, Equation (10) is first substituted into Equation (6). To perform the integration, Kihara arbitrarily fixed the orientation of both molecules. He then allowed one molecule core to move over all points of the surface of the second which remains in the fixed orientation. Next he considered the second molecule in all possible orientations. Finally through the use of some topological and averaging theorems Kihara arrived at the following expression for $B(T)$:

$$B(T) = b_0 F_1 + M_0 \rho_0^2 F_2 + \rho_0 (S_0 + (1/4)M_0^2) F_3 + V_0 + (1/4)M_0 S_0 \quad (E-3)$$

where $b_0 = (2/3)\pi N \rho_0^3$ and ρ_0 is defined as in Chapter II, M_0 is the surface integral of the mean curvature of the

core over the core surface and is given for smooth curved surfaces by:

$$M_0 = \int_S 1/2(1/R_1 + 1/R_2) dS \quad (E-4)$$

where R_1 and R_2 are the principle radii of curvature. V_0 and S_0 are the surface volume and area respectively. An extensive tabulation of F_1 , F_2 , and F_3 as a function of $1/T^*$ is available (9).

Method of Least Squares

The method of least squares was used to obtain the best fit of the experimental data to either equation E-1, E-2, or E-3. The procedure used for the Lennard-Jones potential is as follows:

$$B = b_0 B^*(T/\epsilon/k) \quad (E-5)$$

Assuming $(b_0)_0$ and $(\epsilon/k)_0$ and knowing the function B^* and T one can calculate a B , ie, B_{calc} . Then let

$$R_i = (B_{calc})_i - (B_{obs})_i \quad (E-6)$$

where $(B_{obs})_i$ is the experimentally determined second virial coefficient and i refers to the temperature point. Next B is expanded in a first order Taylor series

$$(B_{calc})_i = (B_{obs})_i + \alpha \left(\frac{\partial B}{\partial b_0} \right)_i + \beta \left(\frac{\partial B}{\partial (\epsilon/k)} \right)_i \quad (E-7)$$

if λ_i is defined as

$$\hat{v}_i = (B_{\text{calc}})_i - (B_{\text{obs}})_i + \alpha \left(\frac{\partial B}{\partial b_0} \right)_i + \beta \left(\frac{\partial B}{\partial (\epsilon/k)} \right)_i \quad (\text{E-8})$$

or

$$\hat{v}_i = R_i + \alpha \left(\frac{\partial B}{\partial b_0} \right)_i + \beta \left(\frac{\partial B}{\partial (\epsilon/k)} \right)_i \quad (\text{E-9})$$

The least squares analysis minimizes \hat{v}_i^2 or indirectly R_i . This is accomplished by taking the first derivatives of \hat{v}_i^2 and setting them equal to zero as follows:

$$\sum_i \frac{\partial \hat{v}_i^2}{\partial \alpha} = 0 = \sum_i \left[R_i + \alpha \left(\frac{\partial B}{\partial b_0} \right)_i + \beta \left(\frac{\partial B}{\partial (\epsilon/k)} \right)_i \right] \left(\frac{\partial B}{\partial b_0} \right)_i \quad (\text{E-10})$$

and

$$\sum_i \frac{\partial \hat{v}_i^2}{\partial \beta} = 0 = \sum_i \left[R_i + \alpha \left(\frac{\partial B}{\partial b_0} \right)_i + \beta \left(\frac{\partial B}{\partial (\epsilon/k)} \right)_i \right] \left(\frac{\partial B}{\partial (\epsilon/k)} \right)_i \quad (\text{E-11})$$

These two equations are solved for α and β which then are used with the following equations to calculate new estimates of ϵ/k and b_0 :

$$\epsilon/k = (\epsilon/k)_0 + \alpha \quad (\text{E-12})$$

and

$$b_0 = (b_0)_0 + \beta \quad (\text{E-13})$$

The above procedure is repeated until values of ϵ/k and b_0 are obtained which make the following quantity a minimum:

$$\sum R_i = \text{minimum} \quad (\text{E-14})$$

The following procedure was used to obtain B_{calc} , $\frac{\partial B}{\partial b_0}$, and $\frac{\partial B}{\partial (\epsilon/k)}$ in this work:

From the known temperature, T , and an initial estimate of ϵ/k , $(T^*)_0$ is calculated. The tabulated T^* just below the calculated value and the two values just above the calculated value were used to calculate the constants in the following equation:

$$B^*(T^*) = C_1 + C_2(1/T^*) + C_3(1/T^*)^2 \quad (\text{E-15})$$

This equation was used to calculate B_{calc} at $(T^*)_0$. The above equation was differentiated to obtain the derivatives. This is not the most accurate method but since the derivatives are used only to arrive at new estimates of ϵ/k and b_0 , this method was found to suffice. In the case of the Kihara potential the derivative $\frac{\partial B}{\partial b_0}$ was replaced by $\frac{\partial B}{\partial \rho_0}$. Also F_1 , F_2 and F_3 were calculated using an equation similar to Equation E-15.

For the Stockmayer potential it was necessary to interpolate between the tabulated values of t^* . An equation similar to E-15 was used for this interpolation.

This procedure of using a quadratic exact fit around the value $(T^*)_0$ was employed after it was found that fitting the tabulated values of $B^*(T^*)$ to a polynomial of $1/T^*$ gave unsatisfactory results.

VITA

David Harrison Knoebel

Candidate for the Degree of

Doctor of Philosophy

Thesis: SECOND VIRIAL COEFFICIENTS OF SEVERAL POLAR-
NONPOLAR BINARY MIXTURES

Major Field: Chemical Engineering

Biographical:

Personal Data: Born in Glenwood City, Wisconsin,
January 7, 1940, the son of Harrison J. and Emma
M. Knoebel.

Education: Attended elementary school in Glenwood
City, Wisconsin; graduated from Glenwood City
High School in 1957; received the Bachelor of
Science degree in Chemical Engineering from
Michigan College of Mining and Technology at
Houghton, Michigan in 1961; received the Master
of Science degree in Chemical Engineering from
Oklahoma State University at Stillwater,
Oklahoma in 1964; completed requirements for
the Doctor of Philosophy degree in May 1967.

Professional Experience: Employed as a student aide
with Argonne National Laboratory in the Summer
of 1960; employed as an engineering trainee
with DuPont Savannah River Laboratory in the
Summer of 1961; employed in the Summer of 1963
as an engineer (temporary) with Standard Oil
Company of California; presently employed as a
research engineer with DuPont Savannah River
Laboratory.